

DLR-IB-FA-BS-2016-173

**Design rules consideration within
optimization of composite
structures using lamination
parameters**

Masterarbeit

Edgar Werthen, Sascha Dähne



DLR

**Deutsches Zentrum
für Luft- und Raumfahrt**

Institut für Faserverbundleichtbau und Adaptronik

DLR-IB-FA-BS-2016-173

**Design rules consideration within optimization
of composite structures using lamination
parameters**

Zugänglichkeit:

Stufe 1 (intern und extern unbeschränkt zugänglich)

Braunschweig, 08, 2016

Der Bericht umfasst: 69Seiten

Institutsleiter:

Autoren: *Edgar Werthen*

Prof. Dr.-Ing. M. Wiedemann

Betreuer: *Sascha Dähne*

Abteilungsleiter:

Prof. Dr.-Ing. Christian Hühne



**Deutsches Zentrum
für Luft- und Raumfahrt**



University of applied sciences of Landshut and Ingolstadt
European school of CAE technology
German Aerospace Center (DLR)

Master of applied computational mechanics (ACM)

MASTER THESIS

Design rules consideration within optimization of composite structures using lamination parameters

Author: **Edgar Werthen**
Technical supervisor: **Sascha Dähne**
First examiner: **Prof. Dr.-Ing. Christian Hühne**
Second examiner: **Prof. Dr.-Ing. Otto Huber**

Issued on: **01/02/2016**
Submitted on: **28/07/2016**

Declaration

I hereby declare that this thesis is my own work, that I have not presented it elsewhere for examination purposes and that I have not used any sources or aids other than those stated. I have marked verbatim and indirect quotations as such.

Date

Edgar Werthen

Content

Symbols and Units	III
Indices.....	IV
Terms and Abbreviations	IV
1. Introduction and problem description	1
2. Design rules for composite structures	4
2.1 Aircraft industry.....	4
2.2 Wind power industry.....	10
2.3 Selection of design rules.....	12
3. Gradient-based optimization of composites using lamination parameters	13
3.1 Constitutive equations of a laminated composite plate	13
3.2 Lamination parameters	14
3.3 Gradient-based optimization	17
3.3.1 Physical example	17
3.3.2 Mathematical formulation	18
3.3.3 General optimization procedure	19
3.4 Feasible domain.....	21
3.4.1 General description	21
3.4.2 Special case for 0° , $\pm 45^\circ$ and 90° plies.....	22
3.5 Optimization with lamination parameters.....	27
3.5.1 Optimization problem	27
3.5.2 Determination of the gradients.....	30
3.5.3 Selection of the optimizer	31
3.5.4 Convergence criteria	32
3.5.5 Optimization process.....	33
3.6 Conversion from LPs to a laminate configuration.....	34
4. Implementation of design rules in the optimization algorithm	35
4.1 State of the art	35
4.2 A modified design criterion	38
4.3 Assembly constraints formulation	39
4.3.1 Approach	39
4.3.2 Mathematical formulation	40
4.3.3 Results of the parameter study	42
4.4 Comparison to Macquart's constraints	45

4.5	Assembly constraints implementation.....	47
5.	Application of an example.....	48
5.1	Model and material definition	48
5.2	Reference results.....	49
5.3	Results under consideration of assembly constraints.....	51
5.4	Conversion to discrete stacking sequences.....	53
6.	Conclusion and Outlook	56
7.	References.....	58
8.	Appendix.....	60
8.1	List of figures	60
8.2	List of tables.....	61

Symbols and Units

Table 1-1: List of Symbols and Units

Symbol	Description	Unit
$[0_3, 90_2]_s$	Symmetric laminate with 6 0° and 4 90° plies	
$[A]$	Extensional stiffness matrix	N/mm
$[B]$	Extension – bending coupling matrix	N
$[D]$	Bending stiffness matrix	Nmm
E	Elastic modulus	N/mm ²
G	Shear modulus	N/mm ²
L	Minimum step length between two terminating plies	mm
N	Total number of plies	
Q_{ij}	Matrix entries of the reduced stiffness matrix of a lamina	N/mm ²
$\bar{Q}_{ij,k}$	Matrix entries of the reduced stiffness matrix of the k th ply transformed into the global coordinate system	N/mm ²
T	Total laminate thickness	mm
U_1	First material invariant	
$V_{[1,2]}^{*A}$	In-plane lamination parameter 1 and 2, normalized by the laminate thickness	
X	Number of removed plies	
a	Panel length	mm
b	Panel width	mm
h	Step size	
$\{\hat{n}\}$	In-plane forces (per unit length)	N/mm
$\{\hat{m}\}$	Out-of-plane moments (per unit length)	N
t_0	Thickness of one laminate ply	mm
$\{x^q\}$	Vector of design variables of the q-th iteration	
$g(\{x\})$	Constraint function	
z	Thickness coordinate of the k-th ply	
$\{\varepsilon\}$	Strains	
$\{\kappa\}$	Curvatures	
ρ	Density	g/mm ³
σ	Stress	N/mm ²
ν	Poisson's ratio	
θ	Ply angle	°

Indices

Table 1-2: Indices

Index	Description
1,2,3	Lamina (local) coordinates, with 1 along fiber direction
k	Ply index
x, y, z	Laminate (global) coordinates
$crit$	Critical
opt	Optimum value
$stacking$	Value that belongs to a discrete stacking

Terms and Abbreviations

Table 1-3: Terms and abbreviations used

	Description
CLT	Classical laminate theory
LP	Lamination parameter
RF	Reserve factor
VErSO	Virtual Environment for Structural Optimization
UD	Fabric with unidirectional fibers
Biax	Fabric with bi-axial fibers
Triax	Fabric with tri-axial fibers

1. Introduction and problem description

Endless fiber-reinforced plastics are used in structures which require a high stiffness-to-weight as well as strength-to-weight ratio such as aircraft wings or wind turbine blades. The idea is to design the structure in a way that it meets the functional requirements combined with a high utilization of the material. Thereby the directional properties of the composite material are used to tailor the structural performance in a principle direction where it is needed. One example for a performance requirement would be the global bending stiffness of a wind turbine blade to restrict the deformation towards the tower. A uniform stiffness in all directions (e.g. in case of steel) would lead to an oversizing of the structure in the non-principle directions. The design variables that influence the structural performance are the ply counts of a given material and the ply orientation angle which form together with the through-the-thickness position the so-called “stacking sequence” of a laminate. Changing the stacking sequence for a fixed overall laminate thickness can lead to a different bending behaviour.

The structural performance can be evaluated with the help of finite element models that are used to proof whether selected failure criteria for composites are satisfied. Failure criteria in this context describe the failure modes of composites for strength (ply based stress criteria) and buckling stability. Such criteria drive the design in a direction that it does not fail.

To support the designer utilizing the composite material strengths best possible on the one side and to handle its weakness on the other side, design rules have been developed during the last decades. These guidelines are based on results from prototype tests and industrial experience. The intention of using design rules is to avoid the occurrence of critical failure modes e.g. delamination and simultaneously guarantee a manufacturable design. They are usually defined based on ply level in thickness or in longitudinal direction. One example rule in thickness direction is the usage of only laminates that are symmetric about their mid-plane which leads to restrictions in the stacking sequence. One important design rule in longitudinal direction is the continuity of plies between two neighbouring panels to ensure the manufacturability. The terms “panel” and “laminate” are used synonymous and subsidiary for a component with the same laminate material properties.

Due to the fact that the structural performance is driven by several influential variables and the design has to fulfill different failure criteria and design rules, a parametric description of the design process is useful and has major advantages. It allows the usage of mathematical optimization with the influence quantities as design values and the failure criteria as constraints which brings the design process into a systematic and well-organized form.

There are several optimization procedures available for composite structures based on either discrete (e.g. ply angles and position of a discrete set) or continuous design variables (e.g. thickness). Usually the laminate stiffness is described by the thickness and the stacking sequence that has a non-linear influence on the structural deformation. An alternative is to formulate the stiffness as a linear combination of the material invariants and the so-called “lamination parameters” which characterize laminate configurations (ply angles and thicknesses) and have a linear dependency regarding the laminate stiffness.

The lamination parameters replace the trigonometric functions and therefore represent the laminate stacking. The avoidance of the trigonometric functions leads to a convex lamination parameter space, which makes the 12 lamination parameters suitable as continuous design variables in a gradient-based optimization process. In case of laminates with more than 13 plies the number of design variables can be reduced significantly when using lamination parameters and the laminate thickness instead of ply

orientations. Regarding the application of the already mentioned design rule for the usage of only symmetric laminates allows a reduction to 8 lamination parameters which further decreases the number of design variables.

The above mentioned design rules can also be implemented in an optimization process. Due to their definition based on ply level, several rules are already mathematically formulated as design criteria to make them appraisable. Based on the criteria constraints are derived for an optimization with the stacking sequence as discrete design variables. One important criterion is the stacking sequence continuity developed by Liu et al. [1] which is a measure of continuous plies between two adjacent laminates respectively two neighbouring optimization regions. A ply is defined to be continuous when it occurs in both laminates and is separated in thickness direction by only one terminated ply. Thereby it does not matter if the terminated ply is part of the thinner or thicker laminate. A further approach to obtain a certain degree of ply continuity is the so called “laminate blending” introduced by Adams et al. [2]. A laminate of two panels is blended outwardly (or inwardly) if the stacking of panel 2 is obtained by removing the outermost (or innermost) plies of panel 1. To generate a globally blended structure a genetic algorithm is used to find an optimal stacking guide for the complete structure. The stacking guide represents the thickest panel and all other panels of the structure are obtained by dropping plies from it.

To the best of the authors’ knowledge the only existing approach, that takes into account blending constraints in lamination parameter space for continuous optimization is the one developed by Macquart et al. [3]. His approach is based on an analytical formulation of blending constraints for laminates, in which all plies have the same orientation angle (extreme laminates). With the help of this extreme value analysis it turns out, that the allowable change of a single lamination parameter is mostly driven by the taper ratio (number of removed plies over all plies) and not by the blending itself. Therefore the obtained feasible domain for the allowable change in lamination parameter space, when removing plies from the thicker laminate, seems to be too large as will be shown within the present work.

In commercial sizing tools like HyperSizer [4] the consideration of design rules is usually a downstream process and is based also on discrete stacking sequences. The sizing process itself returns the target thickness and the percentage of different ply orientations. Based on this data discrete stacking sequences are derived by manually shuffling the stackings in order to fulfill several design rules.

The goal of the present thesis is to formulate a design criterion based on selected design rules in thickness as well as in longitudinal direction. The selection of the design rules is done in accordance with their importance and the feasibility of the implementation into an optimization process. A design criterion is an appraisable quantity and is used to derive constraints for a gradient-based optimization with lamination parameters as continuous design variables for a pre-defined set of ply angles. These constraints should restrict the feasible domain of the laminate parameter space in a way that selected design rules are fulfilled.

The mentioned design criteria of Liu et al. [1] and Adams et al. [2] (developed for discrete stacking sequences to guarantee ply continuity) serve as a basis to formulate a modified criterion for the lamination parameter space as a mixture between laminate blending, stacking continuity and a required taper slope. It is important to note that this design criterion brings out so called “assembly constraints” that interrelate the design variables of two adjacent but different panels to each other. The design rules concerning symmetric and balanced laminates are also treated as a criterion to restrict the lamination parameter space of each individual panel. The assembly constraints are implemented in a gradient-based

optimization process called “VERSO” (Virtual Environment for Structural Optimization), which was developed in cooperation with Mr. Sascha Dähne at the DLR Institute of composite structures and adaptive systems in Brunswick.

The present thesis is structured in five sections. A description of the relevant design rules for the sizing and optimization during the preliminary design phase of composite structures used in the aircraft- and wind power industry is given in **section 2**. The selection of relevant design rules that will be implemented in the optimization process is explained. **Section 3** introduces the gradient-based optimization with lamination parameters as continuous design variables. After a short overview of the constitutive equations for a laminated composite plate, a description of the laminate stiffness as function of the lamination parameters and material invariants is given. An introduction into gradient-based optimization is followed by the description of the feasible domain of the LPs as continuous design variables. Section 3 concludes with an overview of the developed optimization process VERSO. State-of-the-art formulations of design criteria are presented in **section 4**. Furthermore the definition of a modified design criterion is given, that combines the approaches from Liu et al. [1] and Adams et al. [2] and make them applicable for the lamination parameter space. Based on this design criterion assembly constraints are formulated to restrict the lamination parameter space of adjacent panels. The application of an assembly with two components is documented in **section 5**. The results with and without assembly constraints are compared and discussed. The thesis concludes with a summary and an outlook presented in **section 6**.

2. Design rules for composite structures

This chapter lists the relevant design rules for the sizing and optimization of endless fiber-reinforced composites used in the aircraft- and wind power industry. Afterwards the selection of the most important design rules is described and their choice is justified. The documentation of the design rules is focused on the preliminary design of large scale and continuous composite structures and has therefore not the right of completeness. Further design rules regarding other topics like bonding, assembling, thermal treatments, testing and repair of composite structures can be found in [5] and [6].

2.1 Aircraft industry

Table 2-1 lists the relevant design rules in thickness direction (z-direction in Figure 2-1) for laminates used in the aircraft industry. The design rules in longitudinal direction (x-direction in Figure 2-1) are given in Table 2-2. More details about the background of each individual design rule can be found in the related reference giving in the last column of the tables.

Symmetric laminates

Laminates that have a stacking of ply angles symmetric to the laminate mid-plane are called symmetric laminates. Within the present work it is assumed that the mid-plane is located between two plies. As described in Niu et al. [5] and the Composite Materials Handbook (MIL-HDBK-17-3F) [6], the main advantage of these laminates is the uncoupling of membrane and bending behaviour of the structure. Analysis and testing like the measurement of stiffness and strength values of the structure can be simplified due to a more predictable deformation behaviour. Furthermore, the tolerance management during the assembly is simplified. The present design rule cannot be always rigorously fulfilled for example in tapering areas where the laminate thickness changes. In case of locally non-symmetric laminates the asymmetric part should be placed as close as possible to the mid-surface to minimize the warping.

Balanced laminates

An extension of the demand for symmetric laminates is the usage of balanced laminates. Balanced in this context indicates that all ply angles other than 0° and 90° should occur in pairs of $+\theta$ and $-\theta$ above and below the mid-surface. Balanced laminates have similar advantages like symmetric ones. One important property is the decoupling of in-plane membrane and shear behaviour of the structure. The two membrane stiffness terms representing this coupling are determined by the summation of the ply stiffness terms that contain products of odd powers of sine and cosine functions as shown by Jones [8]. Therefore 0° and 90° do not contribute to these stiffness terms. If other ply angles $+\theta$ have a partner ply angle $-\theta$ the sum of both results in zero and a contribution is also not given. A further criterion why laminates should be symmetric and balanced is the maximization of buckling strength. As documented in Niu et al. [1] and Jones [8] the membrane-bending and also bending-twisting coupling increase the deformation while decreasing at the same time the buckling resistance and vibration frequencies as it would be expected for panels with a significant lower bending stiffness. An important exception where unbalanced laminates are used is the application of aero-elastic tailoring. One example is a forward swept wing where unbalanced laminates are used to produce a membrane in-plane and shear coupling of the wing skins to avoid an aerodynamic divergence. A further example is an aero-elastic tailored wind turbine blade for which a structural bend-twist coupling is requested to improve locally the angle of inflow.

Outer plies and damage tolerance

Another design rule in thickness direction given in Niu et al. [5] is the placement of $\pm 45^\circ$ plies on the outer laminate surface to increase the damage tolerance and impact resistance e.g. against tool drop. At the same time the load-carrying 0° plies should not be placed at the outer surfaces due to operational aspects. This procedure is recommended for possibly instable laminates to maximize the buckling resistance. The effect can be shown with equation (2-1) [8] for the critical buckling load of a long panel axially loaded.

$$\hat{n}_x = \pi^2 \left[D_{11} \left(\frac{m}{a} \right)^2 + 2(D_{12} + 2D_{66}) \left(\frac{1}{b^2} \right) + D_{22} \left(\frac{1}{b^2} \right) + D_{22} \left(\frac{1}{b^4} \right) \left(\frac{a}{m} \right)^2 \right] \quad (2-1)$$

The variables a and b constitute the panel length and -width and m is the number of half waves of the buckling mode shape in longitudinal direction. It can be observed that \hat{n}_x is a function of four times D_{66} and only one times of D_{11} (respectively D_{22}). Therefore adding $\pm 45^\circ$ plies as far as possible from the mid-surface to increase D_{66} is four times more effective than adding 0° or 90° plies.

Contiguity and maximum ply thickness

This design rule refers to a limitation in the thickness of adjacent plies with the same orientation angle. According to Niu et al. [5] for a laminate with a standard ply thickness of 0.127mm, not more than four contiguous plies are recommended. For thicker plies not more than two plies with the same orientation angle should be staged together. To outline the origin of this design rule a short introduction into inter-laminar stresses is given in the following. As described by Pipe et al. [9] the classical laminate theory (CLT) predicts a state of plane stress for symmetric laminates under traction loads. Each ply has an axial stress σ_x and an in-plane shear stress τ_{xy} as shown in Figure 2-1.

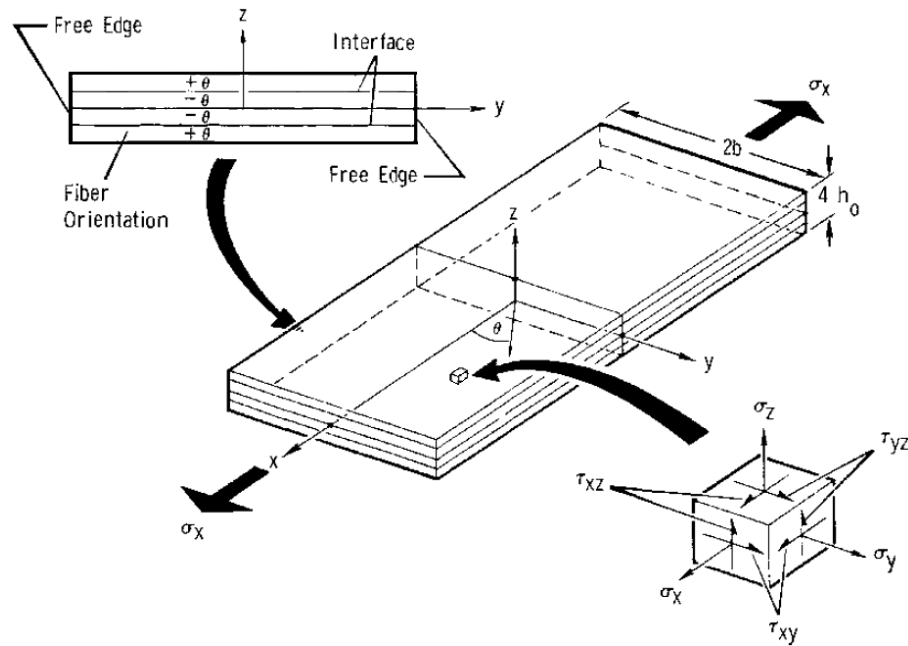


Figure 2-1: Symmetric laminate with four plies under axial loading [9]

The stresses are constant within the ply but vary from one to another ply. The results of the CLT are only exact in case of laminates with infinite widths due to the fact that at the free side edge (Figure 2-1 at $y=b$)

the shear stress τ_{xy} reduces to zero and inter-laminar stresses τ_{xz} , τ_{yz} and σ_z occur in the boundary region.

Figure 2-2 shows the right half of the outer ply extracted as a free body in the y-z plane. The normal stress σ_y is caused by differences in Poisson's ratio and thermal expansion in the x-y plane of the neighbouring ply with a different orientation angle. Its normal force is balanced by the shear force produced by the inter-laminar stress τ_{yz} close to the free edge. Due to the fact that the forces are not collinear a moment arises from this couple of forces. A counter moment arises near the free edge which induces a normal stress couple in z-direction as shown in Figure 2-2. The thicker the ply the greater is the moment (due to the distance between σ_y and τ_{yz}) and the higher are the resulting inter-laminar stresses τ_{yz} and σ_z which can cause transverse cracks or free-edge delamination. Based on these observations the design rule was created to limit the ply thickness respectively the number of plies with the same orientation angle. Exceptions exist for situations where matrices with higher performance are used and the maximum allowable ply thickness can be enlarged.

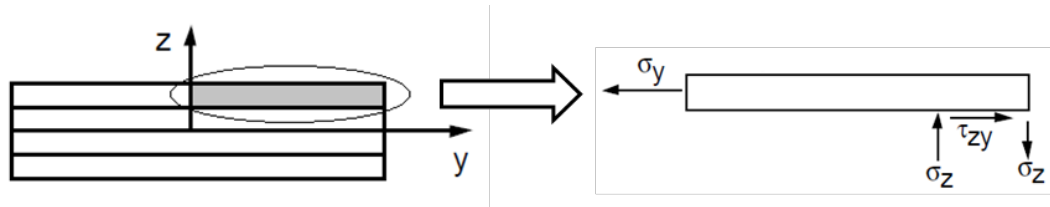


Figure 2-2: Right part of the outer ply extracted as a free body

10%-rule

The so called “10%-rule” refers to the requirement having minimal in-plane stiffness in all fiber directions like 0° , 90° and $\pm 45^\circ$. The goal is to cover secondary loads and to create more robust laminate properties in comparison to highly orthotropic laminates. Furthermore a matrix-dominated behaviour (e.g. nonlinear effects and creeping) can be avoided for laminates where the main fiber direction is not aligned with principle load axis as described in the MIL-HDBK-17-3F [6]. There is no formal documentation of this guideline that confirms its validity, but due to the fact that it has been followed successfully in many production programs it is still present in these days.

Taper slope and maximum thickness step

The first design rule in longitudinal direction of the laminate is the limitation of the taper slope in zones where the plies are dropped off due to thickness variations. As documented in Niu et al. [5] thickness changes lead to discontinuities and eccentricities in the laminate stiffness which can cause inter-laminar failures as described above. Thickness steps along the main load direction should have a taper slope of at least 1:20. In case of a drop of four plies (e.g. 0.508mm) the next ply drop can occur earliest after $20 \times 0.508\text{mm} = 10.16\text{mm}$ in horizontal direction. Thickness changes in other directions should have a taper slope of at least 1:10 which is also valid for stiffeners and beam flange edges. Plies with angles other than 0° and 90° have to be dropped off in $\pm \theta$ pairs in case that unbalanced laminates are not allowed.

According to Niu a single thickness step should not exceed 0.508mm which corresponds to four plies if the ply thickness is 0.127mm. This is the same value as recommended above for the maximum thickness of contiguous plies. The goal is to smooth the load distribution over the structure and to avoid high stress

concentrations (especially inter-laminar stresses) at the ply drop. Further limitations according to dropping of plies are documented in the following.

Ply-drop techniques

Recommended techniques how the ply drops should be arranged are given in [6] and [10]. If possible, ply drops should be arranged symmetric about the laminate mid-plane to achieve an adequate redistribution of the load through the remaining plies, especially the continuous outer plies. Therefore the first ply should be dropped off close to the mid-plane. Several proposals for symmetric ply drop techniques exist and can be found in [10].

Continuity of plies

This design rule is an extension of the rule “Taper slope and maximum thickness step”. At every interface between two adjacent panels, the plies of the respective thinner panel should cover the complete rest of the structure. The goal of this procedure is to ensure the structural integrity and manufacturability of the structure. This rule implies that ply orientation mismatches between adjacent panels like cutting plies between two panels to change their orientations (butt joints), are not allowed to avoid discontinuities in the material and to keep the manufacturing costs low.

Covering plies

The outer plies of a laminate should be continuous over the complete structure and cover the all ply drops to avoid delaminations at the free edges of the ply ends.

Table 2-1: Design rules in thickness direction used in the aircraft industry

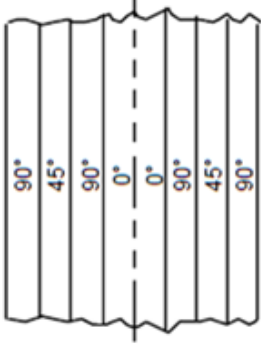

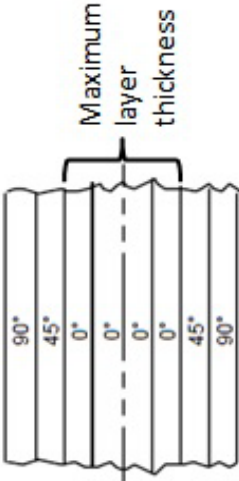
Criterion	Description	Picture	References
Symmetric laminates	The stacking sequence of a laminate should be symmetric about the mid-plane.		[5],[6]
Balanced laminates	The stacking sequence of a laminate should be balanced. Balanced means that the ply angles other than 0° and 90° should appear in pairs of +θ and -θ above and below the mid-plane.		[5],[6]
Outer plies and damage tolerance	To maximize buckling resistance of stability critical laminates, the outer the plies should be ±45° plies. No 0°-ply should be placed on the lower and upper surfaces of the laminate.		[5],[2]
Contiguity and maximum ply thickness	No more than 4 plies (each ply has a max. thickness of 0.127mm) with the same orientation angle should be stacked together. The corresponding maximum thickness of one ply is 0.508mm.		[5],[6]
10%-rule	A minimum of 10% of plies in each of the 0°, ±45° and 90° directions is required.		[5],[6]

Table 2-2: Design rules in longitudinal direction used in the aircraft industry

Criterion	Description	Picture	Reference
Taper slope and maximum thickness step	The taper slope angle in the main load direction should be minimum 1:20 and in other directions 1:10. A single thickness step should not exceed 0.508mm.		[5],[10]
Ply-drop technique	Ply-drops should be arranged symmetrical about the mid-plane. The first ply should drop off close to the neutral axis.		[6],[10]
Continuity of plies	At every interface between two adjacent panels, the plies of the respective thinner panel should cover the complete rest of the structure. Ply orientation mismatches between adjacent panels are not allowed.		[6],[4]
Covering plies	Covering plies on the lower and upper surfaces of the laminate should not be dropped.		[6],[4]

2.2 Wind power industry

Table 2-3 lists the relevant design rules for optimization of composite structures used in the wind power industry. A comparison of the design rules between aircraft industry (documented in [5] and [6]) and the design rules used in the wind power industry shows that the rotor blade guidelines like the DNVGL-ST-0376 [11] have taken over some of the rules in a similar way e.g. the tapering or the continuity of plies. Other rules like the contiguity or the ply drop technique play only a minor role due to the common usage of fabrics and tapes. The demand for symmetric and balanced laminates exists but exceptions are present due to ongoing research on structural bend-twist coupled blades in the current days for example within the Smart Blades project [12]. The design rules used in the wind power industry are described in the following subsections. More details about the background of each individual design rule can be found in the related reference given in the last column of the tables.

Outer plies and damage tolerance

The design rule for outer plies and damage tolerance is taken over from the aircraft industry and adapted for the usage of fabrics. According to Bir et al. [13], the outer plies should be made of Biax or Triax material to provide shear strength and to prevent the inner laminate (unidirectional material) from splaying and buckling. In case of a sandwich structure, the sandwich face is made of Triax plies to transfer the shear loads into the core.

Taper slope and maximum thickness step

In parallel to the aircraft industry the present design rule exists also for the wind power industry. The taper slope has to be calculated specifically based on the shear load criterion to avoid delaminations. Equation (2-2) [11] allows the calculation of the minimum step length L for a ply with the thickness t_0 and an average laminate strength S [N/mm²].

$$L = \frac{S \cdot t_0}{10} \frac{\text{mm}^2}{\text{N}} \quad (2-2)$$

An investigation on delaminations due to ply drops in wind turbine blades has been done by Cairns et al. [14]. According to his results, dropping more than one ply promotes the delamination process as already explained for the covering plies in the previous section. Furthermore inner ply drops are more resistant to delamination due to the double shear surface.

In the DNVGL guideline [11] the tapering criterion is extended for sandwich laminates. The taper slope of core materials should be between 1:3 and 1:10 in the main load direction and between 1:3 and 1:5 in other directions. In the transition region between sandwich core and solid laminate the core material should be tapered with a gradient of maximum 1:3.

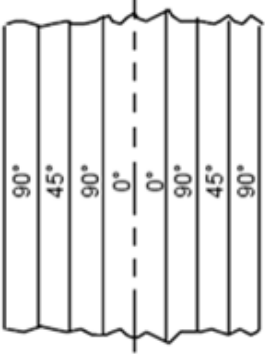
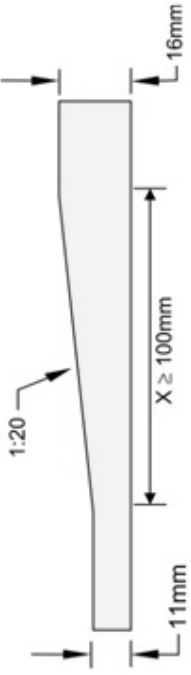
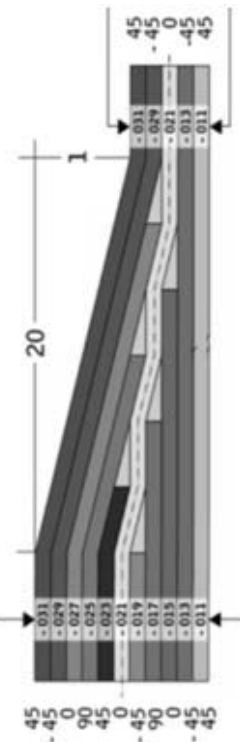
Continuity of plies

The demand for continuous plies is also present in the wind power industry [11] to reduce continuity breaks in the structure and keep the manufacturing costs low. In case that a butt joint is not avoidable at least five undisturbed plies have to be placed in between. Also multiple overlaps should be prevented. Any split of reinforcement plies (e.g. in UD caps) has to be analysed by the designer. Especially for large wind turbine blades the manufacturability of the design is important in terms of production effort and material costs.

Covering plies

The requirement for covering plies over the complete structure is directly taken over from aircraft industry. The goal is to avoid delaminations at the free edges of the ply ends as described by Cairns et al. [14].

Table 2-3 Design rules used in the wind power industry

Criterion	Description	Picture	Reference
Outer plies and damage tolerance	To maximize the buckling resistance of stability critical laminates the outer plies should be Biax or Triax.		[13]
Taper slope and maximum thickness step	The taper slope should be calculated according to the shear load criterion, see equation (2-2).		[11],[14]
Continuity of plies	At every interface between two adjacent panels, the plies of the respective thinner panel should cover the complete rest of the structure. Ply orientation mismatches between adjacent panels are not allowed.		[11]
Covering plies	Covering plies on the lower and upper surfaces of the laminate should not be dropped.		[14]

2.3 Selection of design rules

Comparing the design rules of the aircraft- and wind power industry it can be observed that the intersection of both is given by the following five rules, which are all related to the stacking sequence of a laminate:

1. Symmetric and balanced laminates
2. Outer plies and damage tolerance
3. Taper slope and maximum thickness step
4. Continuity of plies
5. Covering plies

Rule 2 and 5 specify the properties of the outer plies for one laminate and an assembly of minimum two laminates. These rules are not further treated within the present work because their influence on the lamination parameter space can be treated as an offset. In case that an arbitrary laminate stacking has a pair of $\pm 45^\circ$ as covering plies the contribution to its stiffness can be treated as a constant offset which is in case of the bending and coupling matrix ($[D]$ and $[B]$) dependant of the laminate thickness. For the present work the following design rules are selected:

1. Symmetric and balanced laminates
2. Taper slope and maximum thickness step
3. Continuity of plies

The selected rules are present in both industries and have a significant influence on the feasible domain of the lamination parameter space, which will be further explained in section 3.4 and 4.3.

The selected design rules are all based on the discrete stacking sequence. Some of the design rules are already formulated as design criteria to make them appraisable for the optimization with discrete ply angles as design variables. An extract of the state of the art based on a literature research is given in section 4.1. Before that an introduction into gradient-based optimization using lamination parameters as continuous design variables is documented in the following section.

3. Gradient-based optimization of composites using lamination parameters

The goal of the present section is to set up an optimization process for composites with the so called lamination parameters as continuous design variables. The linear mechanical behaviour of a laminated composite plate can be described in a compact form as function of the material invariants and lamination parameters, first introduced by Tsai and Pagano in 1968 [15].

In section 3.1 the constitutive relations of a laminated plate are set up. How they can be reformulated in terms of laminate invariants and the lamination parameters is described in section 3.2. An introduction to gradient-based optimization is given in section 3.3. The geometrical texture and mathematical description of the lamination parameter space is documented in section 3.4. The suitability of the LPs for the application within a gradient-based optimization process is described in section 3.5. The challenging step of converting a laminate parameter set to a feasible stacking is documented in section 3.6.

3.1 Constitutive equations of a laminated composite plate

To set up the constitutive equations of a laminated plate consisting of several unidirectional plies the Classical Laminate Theory (CLT) can be applied. The CLT comprises several assumptions like the plane stress state, small displacements and straight cross section surfaces under deformation.

A loaded laminated plate can be treated as a combined problem of a membrane- and plate element. The cutting forces of an element shown in Figure 3-1 are termed stress resultants with the dimension “force per unit length” (applied force related to the element width). The three in-plane stress resultants are denoted by the vector $\{\hat{n}\}$ and the out-of-plane stress resultants are indicated by the vector $\{\hat{m}\}$.

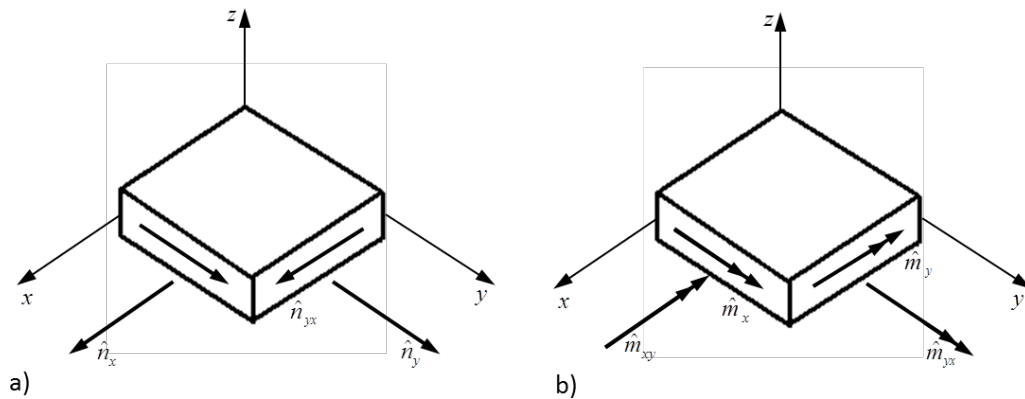


Figure 3-1: Sign convention for the cutting forces on a) the membrane- and b) the plate element

The combined problem allows it to define an extensional stiffness matrix $[A]$ for the membrane element and a bending stiffness matrix $[D]$ for the plate element. Both are coupled with the extension-bending coupling matrix $[B]$. The combination of all three matrices is the global stiffness of the laminate named as “ABD-matrix”. The relation between the stress resultants and the strain vector $\{\epsilon\}$ respectively the vector of curvatures $\{\kappa\}$ is shown in Equation (3-1) which represent the constitutive equations for a laminated plate.

$$\begin{Bmatrix} \{\hat{n}\} \\ \{\hat{m}\} \end{Bmatrix} = \begin{bmatrix} [A] & [B] \\ [B] & [D] \end{bmatrix} \begin{Bmatrix} \{\varepsilon\} \\ \{\kappa\} \end{Bmatrix} \quad (3-1)$$

According to Jones [8] the matrix entries can be calculated with equation (3-2), in which $(\bar{Q}_{ij})_k$ denote the transformed reduces stiffnesses of the k^{th} lamina. “Transformed” in this context refers to the transformation from the local 1,2 coordinate system (with 1 in fiber direction) to the global x-y coordinate system of the laminate. The notation and position of the plies with respect to the laminate middle surface is shown in Figure 3-2.

$$\begin{aligned} A_{ij} &= \sum_{k=1}^N \bar{Q}_{ij,k} (z_k - z_{k-1}) = \sum_{k=1}^N \bar{Q}_{ij,k} t_k \\ B_{ij} &= \frac{1}{2} \sum_{k=1}^N \bar{Q}_{ij,k} (z_k^2 - z_{k-1}^2) = \sum_{k=1}^N \bar{Q}_{ij,k} t_k \left(z_k - \frac{t_k}{2} \right) \\ D_{ij} &= \frac{1}{3} \sum_{k=1}^N \bar{Q}_{ij,k} (z_k^3 - z_{k-1}^3) = \sum_{k=1}^N \bar{Q}_{ij,k} \left(t_k \left(z_k - \frac{t_k}{2} \right)^2 + \frac{t_k^3}{12} \right) \end{aligned} \quad (3-2)$$

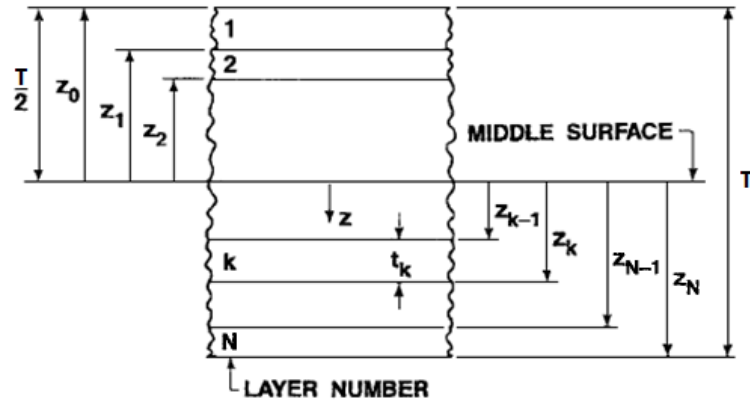


Figure 3-2: Ply numbering and -positioning within the laminate

3.2 Lamination parameters

This section introduces the lamination parameters (LPs) according to the notation used by Tsai and Pagano [15]. The goal is to define the laminate stiffness as a linear combination of the material invariants and the LPs to use them as continuous variables in a gradient-based optimization. As shown in equation (3-2) the matrix entries of the ABD-matrix are build up based on the reduced stiffness of each single ply. As example the matrix entry A_{11} is the sum of the products of $\bar{Q}_{11,k}$ and the related ply thickness for every laminae k . \bar{Q}_{11} can be splitted into three parts like derivated by Jones [8] and shown in Figure 3-3. One constant part U_1 not affected by the orientation angle θ and two frequency components $U_2 \cos(2\theta)$ and $U_3 \cos(4\theta)$ varying with θ .

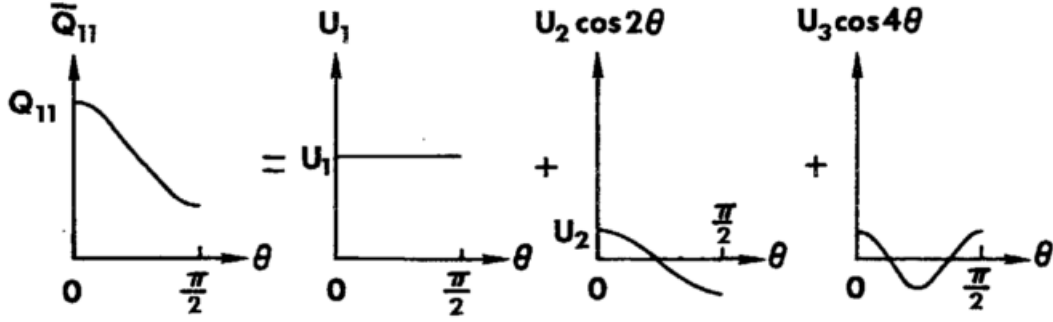


Figure 3-3: Decomposition of the reduced stiffness component [8]

U_1 to U_5 denote the five material invariants calculated with the single, non-transformed material stiffnesses Q_{ij} as shown in equation (3-3).

$$\begin{aligned}
 U_1 &= \frac{1}{8}(3Q_{11} + 3Q_{22} + 2Q_{12} + 4Q_{66}) \\
 U_2 &= \frac{1}{2}(Q_{11} - Q_{22}) \\
 U_3 &= \frac{1}{8}(Q_{11} + Q_{22} - 2Q_{12} - 4Q_{66}) \\
 U_4 &= \frac{1}{8}(Q_{11} + Q_{22} + 6Q_{12} - 4Q_{66}) \\
 U_5 &= \frac{1}{8}(Q_{11} + Q_{22} - 2Q_{12} + 4Q_{66})
 \end{aligned} \tag{3-3}$$

Finally A_{11} can be calculated with the following equation:

$$A_{11} = \sum_{k=1}^N \bar{Q}_{11,k} (z_k - z_{k-1}) = \sum_{k=1}^N (U_1 + U_2 \cos(2\theta_k) + U_3 \cos(4\theta_k)) (z_k - z_{k-1}) \tag{3-4}$$

In case that all plies have the same material and thickness, the invariants can be brought outside the summation. In the following equation the cosine terms are replaced by the first two lamination parameters V_1 and V_2 .

$$\begin{aligned}
 A_{11} &= U_1 \sum_{k=1}^N (z_k - z_{k-1}) + U_2 \underbrace{\sum_{k=1}^N \cos(2\theta_k) (z_k - z_{k-1})}_{V_1} + U_3 \underbrace{\sum_{k=1}^N \cos(4\theta_k) (z_k - z_{k-1})}_{V_2} \\
 &= U_1 T + U_2 V_1 + U_3 V_2
 \end{aligned} \tag{3-5}$$

The same procedure can be done for the other matrix entries of the $[A]$, $[B]$ and $[D]$ matrices. In total 12 lamination parameters together with the material invariants are required to describe the stiffness behaviour of a laminated composite. The 12 LPs normalized to the total laminate thickness T are listed in equation (3-6).

$$\begin{aligned}
V_{[1,2,3,4]}^{*A} &= \frac{1}{T} \sum_{k=1}^N (z_k - z_{k-1}) \cdot [\cos(2\theta_k), \cos(4\theta_k), \sin(2\theta_k), \sin(4\theta_k)] \\
V_{[1,2,3,4]}^{*B} &= \frac{1}{T^2} \sum_{k=1}^N (z_k^2 - z_{k-1}^2) \cdot [\cos(2\theta_k), \cos(4\theta_k), \sin(2\theta_k), \sin(4\theta_k)] \\
V_{[1,2,3,4]}^{*D} &= \frac{4}{T^3} \sum_{k=1}^N (z_k^3 - z_{k-1}^3) \cdot [\cos(2\theta_k), \cos(4\theta_k), \sin(2\theta_k), \sin(4\theta_k)]
\end{aligned} \tag{3-6}$$

The definition of the stiffness entries as a function of the lamination parameters and the material invariants are given in equation (3-7).

$$\begin{Bmatrix} A_{11}, B_{11}, D_{11} \\ A_{22}, B_{22}, D_{22} \\ A_{12}, B_{12}, D_{12} \\ A_{66}, B_{66}, D_{66} \\ A_{16}, B_{16}, D_{16} \\ A_{26}, B_{26}, D_{26} \end{Bmatrix} = \left[T, \frac{T^2}{4}, \frac{T^3}{12} \right] \begin{bmatrix} 1 & V_1^{*A,B,D} & V_2^{*A,B,D} & 0 & 0 \\ 1 & -V_1^{*A,B,D} & V_2^{*A,B,D} & 0 & 0 \\ 0 & 0 & -V_2^{*A,B,D} & 1 & 0 \\ 0 & 0 & -V_2^{*A,B,D} & 0 & 1 \\ 0 & V_3^{*A,B,D}/2 & V_4^{*A,B,D} & 0 & 0 \\ 0 & V_3^{*A,B,D}/2 & -V_4^{*A,B,D} & 0 & 0 \end{bmatrix} \begin{Bmatrix} U_1 \\ U_2 \\ U_3 \\ U_4 \\ U_5 \end{Bmatrix} \tag{3-7}$$

Applying some of the design rules discussed in section 2, the set of individual LPs can be reduced. In case that the laminate is symmetric, the four LPs of the $[B]$ -matrix vanish. Is the laminate in addition balanced according to its mid-plane, the third and fourth LPs $V_{[3,4]}^{*A}$ for the $[A]$ -matrix are zero. 0° and 90° plies have no contribution to the sum of sine functions. Pairs of angled plies cancel out each other due to the anti-symmetry of the sine function with respect to the ordinate. Is the set of allowable ply angles reduced to $0^\circ, \pm 45^\circ$ and 90° plies the fourth LPs are zero, due to the factor 4 within the sine function. As shown in equation (3-7) the LP $V_{[3]}^{*D}$ is only part of the bend-twist coupling terms of the $[D]$ -matrix D_{16} and D_{26} . These terms do not have a contribution to the selected analytical failure criteria for buckling given in equations (3-43) and (3-46) and therefore the $V_{[3]}^{*D}$ parameter is neglected. The remaining four LPs that describe a symmetric and balanced stacking and serve as design variables within an optimization process are $V_{[1,2]}^{*A,D}$.

It can be summarized that the originally non-linear relationship between laminate stiffness and a discrete stacking sequence becomes linear when replacing the trigonometric functions by the lamination parameters like done in equation (3-4). In comparison to the discrete stacking sequence the lamination parameters can be used as continuous and dimensionless design variables within a gradient-based optimization process as described in the following sections. The number of individual LPs could be reduced to four when following the design rules for symmetric and balanced laminates with an even number of plies. Together with the laminate thickness five continuous design variables are needed to describe an arbitrary stacking sequence of a laminate.

3.3 Gradient-based optimization

Numerical optimization, as part of the virtual prototyping process, plays an important role in the design of composite structures. Virtual prototyping is used to reduce the number of physical experiments on prototypes by replacing them with numerical models which describe the design with the design variables. Usually the design process of a composite structure is too complex to describe it with an analytical formulation. As explained by Vanderplaats [16], the analysis of all design variations based on the approach “try them all” is very expensive in computational cost especially with a high amount of design variables. Over the last years a high number of algorithms have been developed to solve numerical optimization problems that describe an automatized design process. Before setting up the mathematical formulation of an optimization problem a physical example is given in the following section.

3.3.1 Physical example

A physical example for an optimization problem is described by Vanderplaats [16]. The goal is to find the top of a hill when person stands at the bottom and wears a blindfold as shown in Figure 3-4 (above). The person has to stay within two fences (one curved and one straight) going from the bottom to the top of the hill. The fences constitute the so-called “constraints” within an optimization. The constraints have the task to constrain the feasible region which is in our example the front side of the hill. In principle the person is able to feel the slope by doing small steps in several directions. He could search in the upward direction for the top of the hill where the two fences meet. This process can be described mathematically in a similar way. The starting location of the person is stored in a vector of the geographical coordinates $\{x^0\}$ (design variables). The direction of the steepest ascent is determined by the gradients calculated with the finite difference method (explained in section 3.5.2) and stored in a vector $\{s^0\}$ that indicates the search direction. The search in the steepest ascent direction is stopped either when crossing the top or by hitting a fence as shown in Figure 3-4 (below).

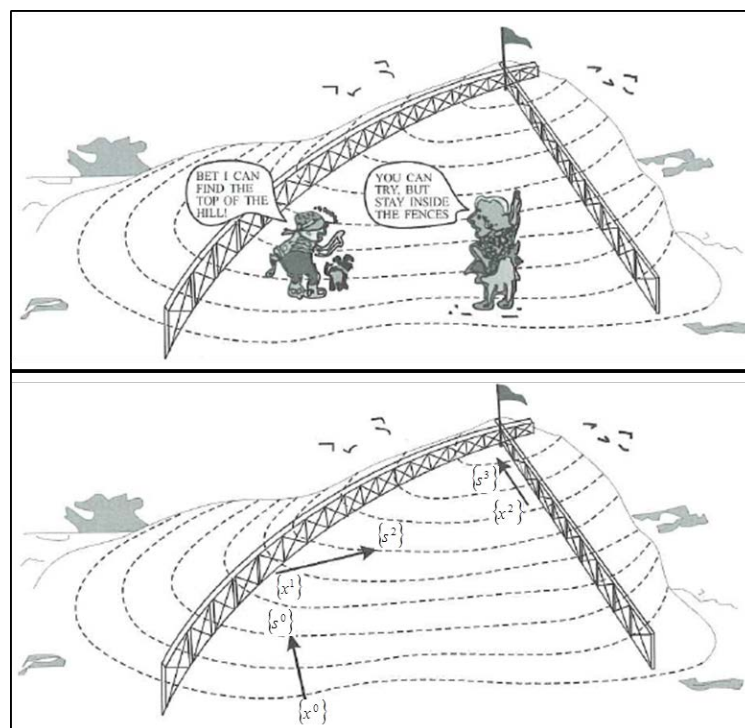


Figure 3-4: Physical example (above) and process (below) for a gradient-based optimization [16]

The location at the fence is denoted by vector $\{x^1\}$ indicating the end of the first iteration. The vector of the design variables is obtained with $\{x^1\} = \{x^0\} + \alpha\{s^1\}$. Now the gradients of the hill and of the fence (outward normal vector) are used to determine a new search direction $\{s^2\}$ which pushes the person away from the curved fence. Going along the fence is not possible because the person can move only along straight lines (direction vectors) as far as possible. The second fence is reached after the second iteration at $\{x^2\}$. Now a search direction $\{s^3\}$ along the straight fence is possible to reach the top of the hill. Indicators that the optimum is found are the zero gradient at the top (only in this example) and the fact that no further search direction going upwards can be found without moving outside the fences.

To set up the mathematical formulation some terms are required which will be introduced based on the described example. The topographical lines (contour lines) constitute the objective function (in this example a quadratic one) where the maximum is searched for. The design variables (geographical coordinates) are allowed to assume values only within the feasible domain. The feasible domain is the area bounded by the constraints that have always be satisfied. In this example the constraints are represented by the two fences (a linear and a non-linear constraint).

3.3.2 Mathematical formulation

The optimization problem described in the previous section is a constrained maximization of the objective function. Of course there are a lot of unconstrained optimization problems which are much easier to solve because their optimum is simply the point where the gradient of the function is zero.

The vector $\{x\}$ describes the design variables with n components out of the domain X . The objective function denoted as $f(\{x\})$ can be constrained inequality constraints $g(\{x\})$ and/or equality constraints $h(\{x\})$. The elements x_i^l, x_i^u of the vector denote the lower and upper boundary values of the design variables and are usually named as side constraints. A standard formulation of the constrained optimization problem is given in the following equation.

Minimize:

$$f(\{x\}) \quad \{x\} \in X \quad (3-8)$$

Such that

$$g_j(\{x\}) \leq 0 \quad j = 1, \dots, m \quad (3-9)$$

$$h_k(\{x\}) = 0 \quad k = 1, \dots, l \quad (3-10)$$

$$x_i^l \leq x_i \leq x_i^u \quad i = 1, \dots, n \quad (3-11)$$

Where

$$\{x\} = \{x_1, x_2, \dots, x_n\}^T \quad (3-12)$$

In case that the objective function should be maximized the same formulation can be used by just minimizing $-f(\{x\})$. The objective function and also the constraints can be linear or non-linear functions of the design variables and can be solved explicitly or implicitly. Therefore their evaluation may be done with any analytical, numerical or even experimental method. For a gradient-based method the objective function and the constraints have to be continuously differentiable with respect to $\{x\}$. The set of design variables out of X for which all constraints are satisfied constitutes the feasible domain. In case that for a

specific design point the equality condition of an inequality constraint holds, the constraints is treated as an active constraint. All satisfied equality constraints are active and all inequality constraints can either be active or inactive in case that they are satisfied with a margin.

3.3.3 General optimization procedure

The goal of this section is to describe the iterative procedure of an optimization algorithm. Based on an initial set of design variables $\{x^0\}$ the design is updated iteratively as given by the following equation [16].

$$\{x^q\} = \{x^{q-1}\} + \alpha \{s^q\} \quad (3-13)$$

q denotes the iteration number, $\{s\}$ the vector in search direction and α the scalar value of the translation along $\{s\}$. Figure 3-5 shows the iterative procedure for a two-variable problem with one search direction. The search direction can be chosen in a way arbitrary with the limitations that the objective function is reduced and no constraint is violated. In the given example the opposite of the gradient of the objective function (steepest descent) is used as search direction which is a typical approach for gradient-based methods. Generally the determination of the search direction is also influenced by the gradients of the constraints at the current design point. The next step is to determine the distance to minimize the objective function without violating any constraint. This is done based on a numerical interpolation scheme. It has to be noted that for this example a one-dimensional search has been applied. The optimum $\{x^*\}$ is only found when a new search direction is determined at the point $\{x^1\}$. Based on the present example the non-linear optimization procedure can be splitted in two parts. One part is the calculation of a search direction that reduces (or increases respectively) the objective function in a way that all constraints are satisfied. The second part is the determination of the scalar parameter α that represents the translation along the search direction.

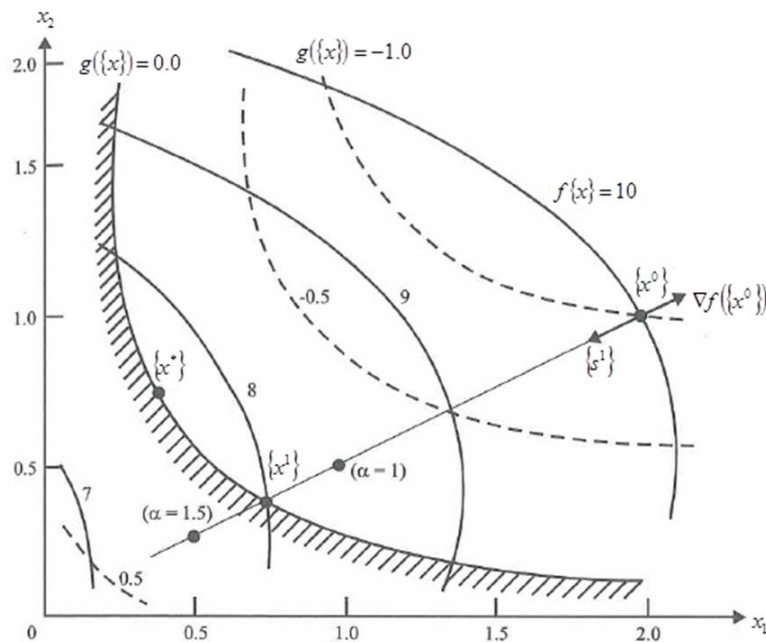


Figure 3-5: Two-variable problem with a one-dimensional search [16]

An important question for the user of an optimization algorithm is, whether the algorithm has found the real optimum or does a better solution exist within the feasible domain.

One practical approach for the proof would be to start the optimization from different initial vectors $\{x^0\}$ and check if the same optimum can be reached. A more reliable approach is to set up mathematical expressions that represent necessary conditions for an existence of an optimum as described in the following. First the concept of convexity is shortly explained as a necessary condition for the existence of an optimum.

A set of points is convex if every point along a line spanned by 2 points of the set is inside the set. In case that any point along the line is outside the set, the set is non-convex. A graphical example is given in Figure 3-6. Any set of lamination parameters form a convex set which denotes the feasible domain as described in the following section.

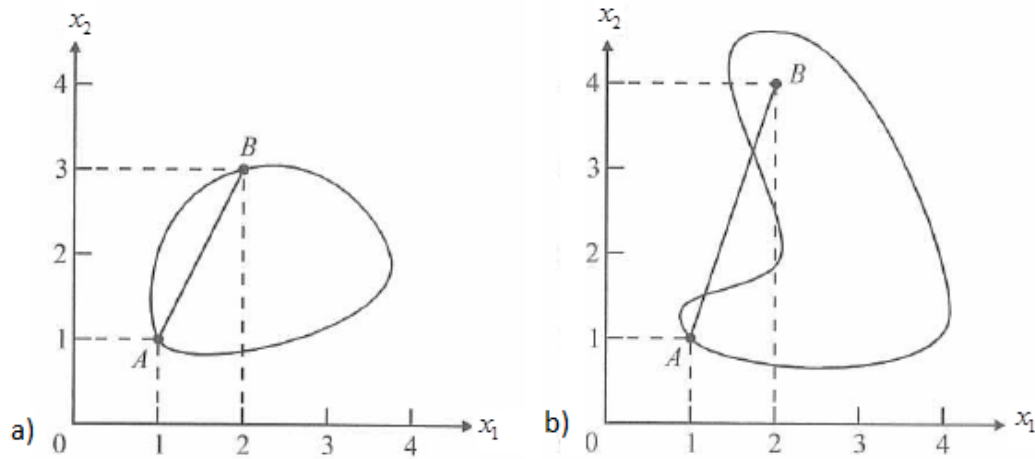


Figure 3-6: A convex (a) and a non-convex (b) set of points

A function is convex between two points $\{x^1\}$ and $\{x^2\}$ if the following equation holds.

$$f(\mu\{x^1\} + (1-\mu)\{x^2\}) \leq \mu f(\{x^1\}) + (1-\mu)f(\{x^2\}) \text{ with } 0 \leq \mu \leq 1 \quad (3-14)$$

One possible proof of the equation is to show the convexity of the constraint function $g(\{x\})$ between the design point $\{x^1\}$ and the optimum $\{x^*\}$ given in Figure 3-5. Furthermore this example shows that if the feasible domain is bounded by a convex objective and convex constraint functions, the design points form a convex set with only one optimum and this is the global one.

3.4 Feasible domain

The goal of the present section is to describe the feasible domain of the lamination parameter (LPs). To use the LPs as continuous design variables in a gradient-based optimization process the feasible domain has to be convex as described in the previous section.

3.4.1 General description

A graphical design procedure which describes the feasible domain of the two in-plane LPs $V_{[1,2]}^{*A}$ was introduced by Miki [17]. Later the procedure was extended by Miki et al. [18] for the two out-of-plane LPs $V_{[1,2]}^{*D}$. A limit value consideration of equation (3-6) indicates the bounds of the LPs with $-1 \leq V_{[1,2]}^{*A,D} \leq 1$. In case that we would consider a laminate with only one fiber orientation angle (extreme laminate) the LPs are $V_1^* = \cos(2\theta)$ and $V_2^* = \cos(4\theta)$. In case that we would vary the fiber angle continuously from 0° to 90° the parabolic boundary line shown in Figure 3-7 is drawn. With the help of the trigonometric identity,

$$\cos^2(2\theta) = \frac{1}{2}(\cos(4\theta) + 1) \quad (3-15)$$

the two in-plane- or out-of-plane LPs can be put into relationship as shown in the following equation.

$$V_2^* = 2V_1^{*2} - 1 \quad (3-16)$$

In case that the laminate has more than one orientation angle, equation (3-16) has to be written as an inequality.

$$V_2^* \geq 2V_1^{*2} - 1 \quad (3-17)$$

The feasible domain of the LPs $V_2^{*A,D} = f(V_1^{*A,D})$ is indicated by the area within the curve ABC, shown in Figure 3-7. The points A, B, C, D and E denotes the laminates with only 0° , $\pm 45^\circ$, 90° , $\pm 30^\circ$ or $\pm 60^\circ$ plies. Choosing a discrete set of orientation angles leads to a different shape and a reduced area of the feasible domain in form of a polygon with vertices located on the perimeter of the feasible domain [18]. Two examples are indicated by dotted lines in Figure 3-7. The set of 0° , $\pm 45^\circ$, 90° plies generates a triangular shape and the set of 0° , $\pm 30^\circ$, $\pm 60^\circ$, 90° brings out a trapezoidal shape of the feasible domain.

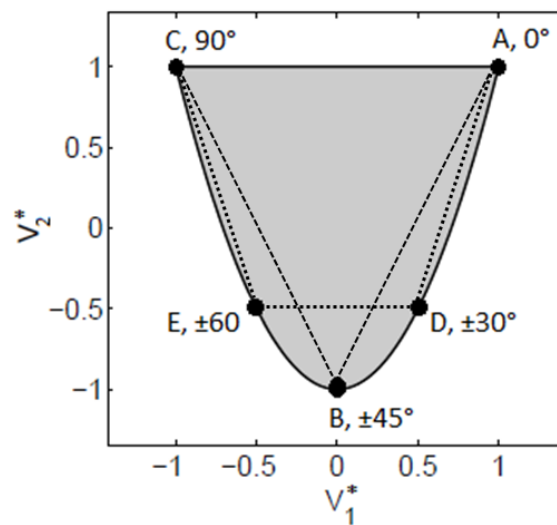


Figure 3-7: Feasible domain for either the in- or out-of-plane LPs

As already indicated in equation (3-6) every LP is a linear combination of volume fractions. Considering a point P on the line \overline{AC} (representing laminates with 0° and 90° plies) at the distance of 0.8 from point A and a total distance between A and C of 2 units, the volume fraction vector can be calculated with the following equation:

$$\{v_p\} = (1-r)\{v_A\} + r\{v_C\} = \left(1 - \frac{0.8}{2}\right)\{1,0\} + \left(\frac{0.8}{2}\right)\{0,1\} = \{0.6, 0.4\} \quad (3-18)$$

In case of a 10 ply laminate point P could correspond to the configuration $[0_3, 90_2]_s$ or any other configuration with the same ratio of 0° and 90° plies. This procedure can be applied to any straight line within the entire feasible domain. Furthermore it indicates that every point can be constructed by multiple pairs of two points which leads to multiple laminates belonging to the same design point in the feasible domain. An example is given in Figure 3-8 where the design point $\{0,0\}$ is constructed by two lines \overline{AE} representing laminates with 0° and $\pm 60^\circ$ plies and \overline{CD} representing laminates with 90° and $\pm 30^\circ$ plies.

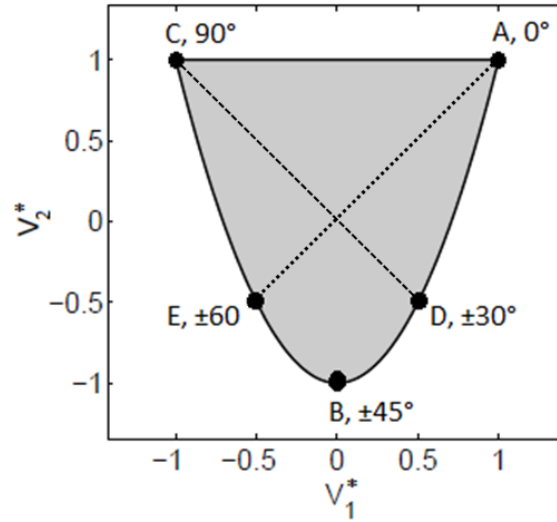


Figure 3-8: Construction of a design point representing multiple laminates

3.4.2 Special case for 0° , $\pm 45^\circ$ and 90° plies

A special case constitutes the feasible domain of laminates with 0° , $\pm 45^\circ$ and 90° plies. Here every design point for the $[A]$ -matrix describes exactly one combination for the counts of 0° , $\pm 45^\circ$ and 90° plies, as shown in Figure 3-9 (left) for a laminate of 4 plies. As already described in section 3.2 the fourth LPs $V_4^{*A,D} = \sin(4\theta)$ vanish due to the fact that the quad of 0° , $\pm 45^\circ$ and 90° is 0° respectively 360° and therefore also the sine of it. The complete feasible domain of any symmetric laminate with ply angles out of the set 0° , $\pm 45^\circ$ and 90° is shown in Figure 3-9 (right).

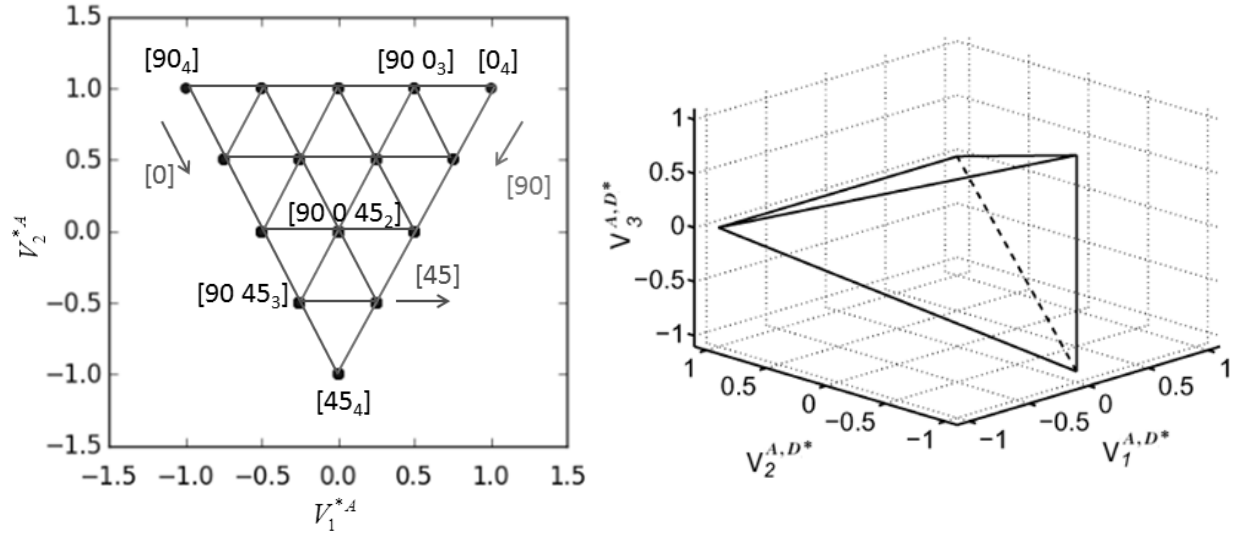


Figure 3-9: Discrete design points of a 4-ply laminate (left), Complete feasible domain of any symmetric laminate with ply angles out of the set of 0° , 45° and 90°

Fukunaga and Sekine [19] defined the analytical relationship between all four in- and all four out-of-plane LPs separately without taking into account the coupling between them. Diaconu et al. [20] found out that the feasible region of any pair of two LPs representing either the $[A]$ -, $[B]$ - or $[D]$ -matrix can be described analytically. Furthermore he presented a variational approach to determine the complete feasible domain for any desired set of LPs numerically. During the variation of a LP set the boundary of the feasible domain is reached by determining a layup function $\theta(\bar{z})$ that maximizes the functional $F[\theta(\bar{z})]$ given in the following equation, where \bar{z} denotes the normalized thickness coordinate $\bar{z} = 2z/T$.

Geometrically the functional F can be interpreted as a constant on a hyperplane with

$$F[\theta(\bar{z})] = \sum_{i=1}^4 k_i^A V_i^A + k_i^B V_i^B + k_i^D V_i^D = \int_0^1 G[\bar{z}, \theta(\bar{z})] d\bar{z}$$

with:

$$G[\bar{z}, \theta(\bar{z})] = \sum_{i=1}^4 g_i(\bar{z}) f_i[\theta(\bar{z})] \quad (3-19)$$

$$g_i(\bar{z}) = \frac{1}{2} k_i^A + k_i^B \bar{z} + \frac{3}{2} k_i^D \bar{z}^2$$

$$f_{[1,2,3,4]}[\theta(\bar{z})] = [\cos 2\theta(\bar{z}), \sin 2\theta(\bar{z}), \cos 4\theta(\bar{z}), \sin 4\theta(\bar{z})]$$

$$\sum_{i=1}^4 \left[(k_i^A)^2 + (k_i^B)^2 + (k_i^D)^2 \right] = 1$$

$\{k\} \equiv \{k_1^A, \dots, k_4^A, k_1^B, \dots, k_4^B, k_1^D, \dots, k_4^D\}^T$ denoting its unit normal. The hyperplane is tangent to a LP set $\{V\}$ touching the boundary of the feasible domain. Increasing F leads to a translation of the hyperplane along the $\{k\}$ direction until F reaches its maximum where the hyperplane touches the boundary line of the feasible region as shown in Figure 3-10.

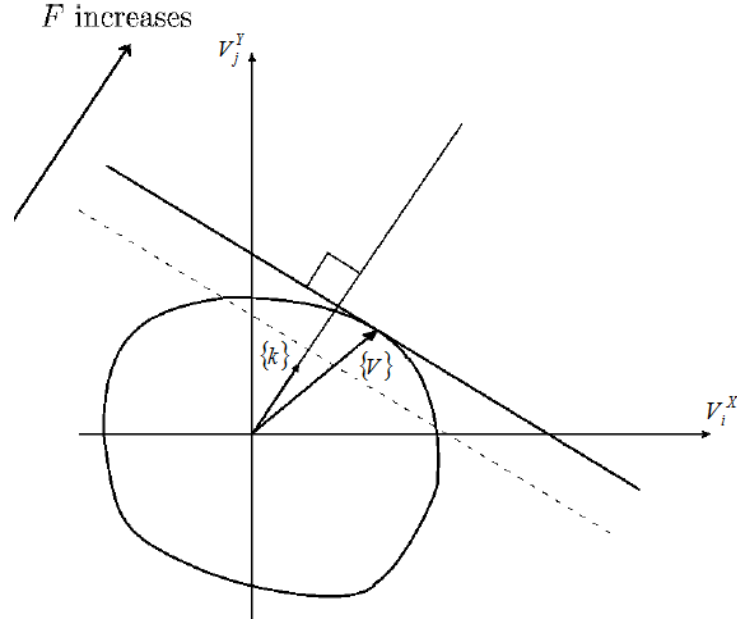


Figure 3-10: Feasible domain of a desired lamination parameter set [20]

Due to the convexity of the feasible domain the boundary can be obtained by determining the hyperplanes for all directions $\{k\}$. This procedure can be done to obtain the feasible domain for any set of LPs without restrictions on potential ply orientations. The detailed mathematical derivation is given in [20].

Diaconu et al. [21] carried out a layup optimization of long composite cylindrical shells. Therefore they derived explicit relations between the LPs to describe the feasible domain based on the developed approach previously described [20]. The ply orientation angles are restricted to 0° , $\pm 45^\circ$ and 90° plies which reduced the number from twelve to nine LPs. The fourth LPs $V_4^{*A,B,D} = \sin(4\theta)$ are zero as already explained.

The linear analytical expressions given in the following equation relating the in- or out-of-plane LPs that form the triangular shape of the feasible domain (see Figure 3-9) were already derived by Fukunaga and Sekine [19].

$$2|V_1^{*A,D}| - V_2^{*A,D} - 1 \leq 0 \quad (3-20)$$

$$2|V_3^{*A,D}| - V_2^{*A,D} - 1 \leq 0 \quad (3-21)$$

Expressions relating the LPs for the coupling were derived by Diaconu et al. based on the method given in [20].

$$2|V_1^{*B}| - |V_2^{*B}| - 2 \leq 0 \quad (3-22)$$

$$2|V_3^{*B}| - |V_2^{*B}| - 2 \leq 0 \quad (3-23)$$

$$|V_1^{*B}| + |V_3^{*B}| - 1 \leq 0 \quad (3-24)$$

The following equations are derived by Diaconu et al. in [21] and [22].

$$4(V_i^{*D} - 1)(V_i^{*A} - 1) \geq (V_i^{*A} - 1)^4 + 3(V_i^{*B})^2, \quad i = 1, 2, 3 \quad (3-25)$$

$$4(V_i^{*D} + 1)(V_i^{*A} + 1) \geq (V_i^{*A} + 1)^4 + 3(V_i^{*B})^2, \quad i = 1, 2, 3 \quad (3-26)$$

$$16(2V_1^{*D} - V_2^{*D} - 1)(2V_1^{*A} - V_2^{*A} - 1) \geq (2V_1^{*A} - V_2^{*A} - 1)^4 + 12(2V_1^{*B} - V_2^{*B})^2 \quad (3-27)$$

$$16(2V_1^{*D} + V_2^{*D} + 1)(2V_1^{*A} + V_2^{*A} + 1) \geq (2V_1^{*A} + V_2^{*A} + 1)^4 + 12(2V_1^{*B} + V_2^{*B})^2 \quad (3-28)$$

$$16(2V_1^{*D} - V_2^{*D} + 3)(2V_1^{*A} - V_2^{*A} + 3) \geq (2V_1^{*A} - V_2^{*A} + 3)^4 + 12(2V_1^{*B} - V_2^{*B})^2 \quad (3-29)$$

$$16(2V_1^{*D} + V_2^{*D} - 3)(2V_1^{*A} + V_2^{*A} - 3) \geq (2V_1^{*A} + V_2^{*A} - 3)^4 + 12(2V_1^{*B} + V_2^{*B})^2 \quad (3-30)$$

$$16(2V_3^{*D} - V_2^{*D} + 1)(2V_3^{*A} - V_2^{*A} + 1) \geq (2V_3^{*A} - V_2^{*A} + 1)^4 + 12(2V_3^{*B} - V_2^{*B})^2 \quad (3-31)$$

$$16(2V_3^{*D} + V_2^{*D} - 1)(2V_3^{*A} + V_2^{*A} - 1) \geq (2V_3^{*A} + V_2^{*A} - 1)^4 + 12(2V_3^{*B} + V_2^{*B})^2 \quad (3-32)$$

$$16(2V_3^{*D} - V_2^{*D} - 3)(2V_3^{*A} - V_2^{*A} - 3) \geq (2V_3^{*A} - V_2^{*A} - 3)^4 + 12(2V_3^{*B} - V_2^{*B})^2 \quad (3-33)$$

$$16(2V_3^{*D} + V_2^{*D} + 3)(2V_3^{*A} + V_2^{*A} + 3) \geq (2V_3^{*A} + V_2^{*A} + 3)^4 + 12(2V_3^{*B} + V_2^{*B})^2 \quad (3-34)$$

$$4(V_1^{*D} - V_3^{*D} - 1)(V_1^{*A} - V_3^{*A} - 1) \geq (V_1^{*A} - V_3^{*A} - 1)^4 + 3(V_1^{*B} - V_3^{*B})^2 \quad (3-35)$$

$$4(V_1^{*D} + V_3^{*D} + 1)(V_1^{*A} + V_3^{*A} + 1) \geq (V_1^{*A} + V_3^{*A} + 1)^4 + 3(V_1^{*B} + V_3^{*B})^2 \quad (3-36)$$

$$4(V_1^{*D} - V_3^{*D} + 1)(V_1^{*A} - V_3^{*A} + 1) \geq (V_1^{*A} - V_3^{*A} + 1)^4 + 3(V_1^{*B} - V_3^{*B})^2 \quad (3-37)$$

$$4(V_1^{*D} + V_3^{*D} - 1)(V_1^{*A} + V_3^{*A} - 1) \geq (V_1^{*A} + V_3^{*A} - 1)^4 + 3(V_1^{*B} + V_3^{*B})^2 \quad (3-38)$$

To proof whether the explicit equations given above completely describe the feasible domain Diaconu worked out an optimization procedure. The method is illustrated in Figure 3-11 where $\{V_0\}$ denotes a potential feasible LP set. A hyperplane $F = \{k\}^T \{V\}$ with $\{k\}$ as its normal vector is tangent to the feasible region. $\{V_Q\}$ marks the intersection point between the elongated feasible LP vector $\{V_0\}$ and the hyperplane F . To proof the feasibility of $\{V_0\}$ the following norm constitutes the objective function to be minimized.

$$D = \left| \{k\}^T \{V\} / \{k\}^T \{\bar{V}_0\} \right| \text{ with } \{\bar{V}_0\} = \{V_0\} / \|\{V_0\}\| \quad (3-39)$$

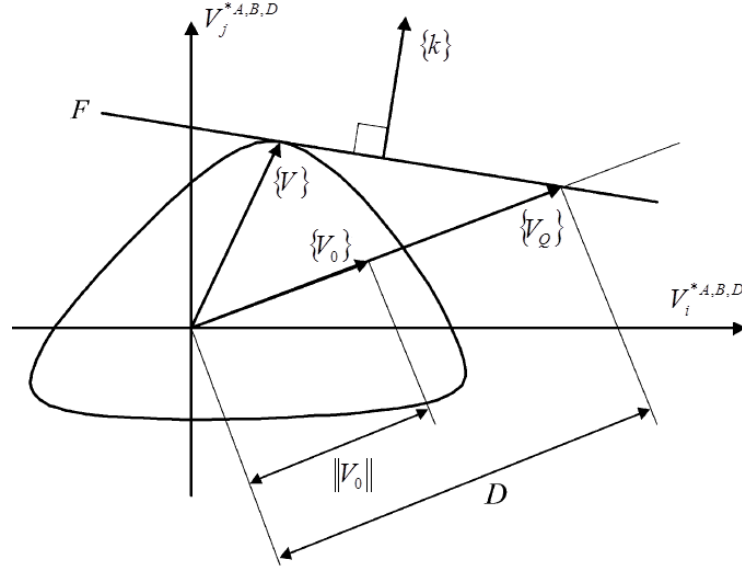


Figure 3-11: Proof if a LP set belongs to the feasible domain [20]

The starting values of the design variables $\{k\}$ are selected in a way that they create a sharp angle with $\{V_0\}$ to have $\{k\}^T \{V_0\} > 0$. The optimization problem can be formulated as follows:

Minimize:

$$D(\{k\}) \quad (3-40)$$

Design variables:

$$\{k\} = \{k_1^A, k_2^A, k_3^A, k_1^B, k_2^B, k_3^B, k_1^D, k_2^D, k_3^D\}^T \quad (3-41)$$

The optimization delivers the optimal $\{V_Q\}$ on the boundary of the feasible region. The feasibility of $\{V_0\}$ is given when $\min D \geq \|\{V_0\}\|$. According to Diaconu this condition is fulfilled for all randomly generated LPs satisfying the constraints giving in equations (3-20) to (3-38). This proves that the constraints are sufficient to describe the feasible domain for the nine LPs $V_{[1,2,3]}^{*A,B,D}$ in case that the ply angles are restricted to 0° , $\pm 45^\circ$ and 90° plies.

The constraints derived by Diaconu given in equation (3-20) to (3-38) represent the feasible domain for a ply angle set of 0° , $\pm 45^\circ$ and 90° . They are used as basis for the gradient-based optimization described in the following section. It has to be noted that only the constraints are used where the four selected LPs $V_{[1,2]}^{*A,D}$ have a contribution. The other LPs are set to zero as described in section 3.2.

3.5 Optimization with lamination parameters

The goal of the present section is to describe the implemented optimization process named VErSO (Virtual Environment for Structural Optimization). The tool is written in the programming language Python. The development of VErSO was done in cooperation with Mr. Sascha Dähne at the DLR Institute of composite structures and adaptive systems in Brunswick. In the first subsection the optimization problem is formulated based on an example with two components. The structural model will be detailed specified in section 5.1. The only relevant information to explain the present process is the number of components. A component specifies a region with the same laminate material properties and is therefore equivalent to an optimization region. In the aircraft industry a wing panel is defined as the area between two rib bays. Within the present work a panel consists of one component.

The terms “panel” and “laminate” are used synonymous and subsidiary for a component. After the mathematical formulation of the optimization problem, VErSO specific properties and processes like the determination of the gradients and the selection of the optimizer itself are documented. The section concludes with a description of the optimization process workflow.

3.5.1 Optimization problem

Before formulating the constrained optimization problem the notation has to be modified in a way that is applicable to multiple components. In the following two indices are used: The first index of $x_{i,2}$ specifies the component number and the second index the design variable number respectively the constraint number.

The objective function that is to be minimized is the overall structural mass of the two components. The mass itself is a linear function of the panel thickness as shown in the following equation. The panel thickness is from now on denoted as the last design variable of a component $\{x_{i,n}\}$.

Minimize:

$$m(\{x_{i,n}\}) = \{c_i\}^T \{x_{i,n}\}, \quad \{x_{i,n}\} \in X \quad (3-42)$$

The vector $\{c_n\}$ represents the constants of the panel like the dimensions and the density. The other four design variables are the reduced set of lamination parameter $V_{[1,2]}^{*A,D}$ due to the restriction on symmetric and balanced laminates with 0° , $\pm 45^\circ$ and 90° plies as described in section 3.2. In total there are ten design variables, five per component (4 LPs and the laminate thickness).

Two different types of constraints are used for the optimization. The constraints that describe the feasible domain for the LPs of each panel are given in equations (3-20) to (3-38). Furthermore the failure criteria compression buckling, shear buckling and strength are considered. The failure criteria are determined analytically. The critical compression buckling load of an axially loaded panel is determined with the following equations [8].

$$\hat{n}_{x,crit} = \pi^2 \left[D_{11} \left(\frac{m}{a} \right)^2 + 2(D_{12} + 2D_{66}) \left(\frac{1}{b^2} \right) + D_{22} \left(\frac{1}{b^2} \right) + D_{22} \left(\frac{1}{b^4} \right) \left(\frac{a}{m} \right)^2 \right] \quad (3-43)$$

$$RF = \frac{\hat{n}}{\hat{n}_{x,crit}} \quad (3-44)$$

$$g(\{x\}) = 1 - \frac{1}{RF} \leq 0$$

RF denotes the reserve factor which is in general the existing stress (respectively strain) over the allowable stress (respectively strain). RF has to be smaller or equal to one. The stiffness values of the $[D]$ -matrix are obtained by multiplying the respective LP with the corresponding material invariant, see equation (3-7). The variables a and b constitute the panel length and -width and m is the number of half waves of the buckling mode shape. The panel length points in the direction of the axial panel load \hat{n}_x .

The critical buckling load for shear is calculated with the VDI guideline 2014-3 [23]. The approach is generally only valued for symmetrical and orthotropic laminates. According to [23] the influence of anisotropy is rated to be small and can therefore be neglected in the preliminary design stage. The bending stiffness of non-symmetric laminates has to be modified with the following equation.

$$[\bar{D}] = [D] - [B]^T [D]^{-1} [B] \quad (3-45)$$

The critical buckling load for shear can be calculated with the following equation.

$$\hat{n}_{xy,crit} = k_s \left(\frac{\pi}{b} \right)^2 \sqrt[4]{\bar{D}_{11} \bar{D}_{22}} \quad (3-46)$$

k_s denotes the buckling factor which is determined based on an approximation method developed by Dähne [24]. The buckling curves are approximated with equations derived from quadratic regression functions in dependency of the modified aspect ratio and Seydel's plate parameter as characteristic value for the orthotropy.

As a constraint for the panel strength the criterion developed by Ijsselmuiden et al. [25] is used. Based on the Tsai-Wu failure criterion the failure envelope equations were formulated. The most important step hereby is the elimination of the ply orientation dependency to obtain functions that describe conservative design envelopes which are convex in the strain envelope. The strength constraint is formulated with a safety factor λ that relates the strain state at the boundary of the envelope P^* to an arbitrary design point P of applied strains as shown in Figure 3-12 and equations (3-47) and (3-48). The safety factor is the inverse of the reserve factor RF . $r(\{\varepsilon\})$ denotes the failure index as function of the strain level which is the reserve factor squared to guarantee the differentiability at all points within the failure envelope.

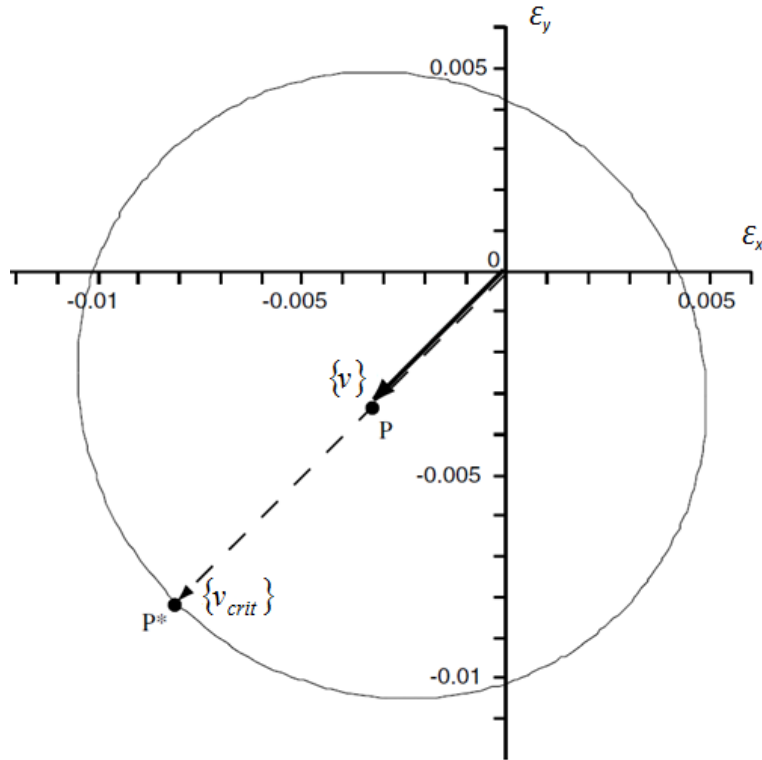


Figure 3-12: Definition of the safety factor for the strength criterion

$$\lambda = \frac{\{v_{crit}\}}{\{v\}} = \frac{1}{RF} \quad (3-47)$$

$$r(\{\varepsilon\}) = \frac{1}{\lambda^2} = RF^2 \quad (3-48)$$

$$r(\{\varepsilon\}) - 1 \leq 0 \quad (3-49)$$

Especially for bending loads the present approximated criterion is more conservative than Tsai-Wu, because the position of plies in thickness direction is not taken into account. In case that sandwich panels are used for bending loaded areas this drawback vanishes because the facesheets are loaded in-plane.

As a last step the upper and lower bounds for the design variables have to be defined. In principle they can be chosen in a way arbitrary. The bounds for the lamination parameter are -1 and 1 as described in 3.4. The bounds for the thickness are chosen based on design or manufacturing rules and practical requirements. As an example when the requirement for symmetrically balanced laminates is present and possible ply angles are 0° , $\pm 45^\circ$ and 90° , the minimum thickness equals to 8 plies. Important criteria for the selection of the minimum skin thickness e.g. for an aircraft wing are the repair strategy, impact and abrasion resistance. The upper bound value for the thickness is restricted among others by the installation space e.g. the aerodynamic hull that represents the outer surface on which the laminate is build-up inwardly. The selected bound values for the given two-component example are shown in the following equations.

$$8t_0 \leq x_{i,n} \leq 30t_0 \quad i = 1, \dots, m \quad (3-50)$$

$$-1 \leq x_{i,j} \leq 1 \quad i = 1, \dots, m, j = 1, \dots, n \quad (3-51)$$

It has to be noted that up to now all constraints are formulated on panel level. Constraints on assembly level will be introduced in section 4.

3.5.2 Determination of the gradients

The calculation of the gradients for the objective function and all constraints at the current design point is necessary to determine the search direction for the next iteration. There are several numerical and analytical methods available. One standard and robust numerical approach which is selected for the present work is the finite difference method. In a further development of the optimization algorithm outside this thesis, analytical approaches could be tested to save computational time. An overview of available analytical methods determining the sensitivity of static response is given by Adelman et al. [26].

The finite difference approximation of a gradient is obtained by truncating the Taylor series representation of the function after the second term. This leads to truncation (discretization) error between the approximation with first-order accuracy and the exact solution. A further error occurs when the computer rounds off decimal quantities e.g. for small step sizes which leads to a loss of precision. The choice of the step size itself constitutes an uncertainty. For the actual implementation of the optimization algorithm the step size is selected individually with 10^{-9} for the laminate thickness (expressed in meters) and 10^{-3} for the LPs.

The process to calculate the gradients can be summarized as follows:

- Vary every design parameter
- Determine the FE solution
- Calculate all constraints for the varied design parameters and compare to the constraints of the originally design parameters
- Form the finite differences based on the following equation

The calculation of the gradients of a function g with respect to every design variable and the step size h is given in the following equations.

$$\{\tilde{x}\} = \{x_{1,1}, x_{1,2}, \dots, x_{i,j} + h, \dots, x_{m,n}\}^T \quad (3-52)$$

$$\frac{dg(\{x\})_k}{dx_{i,j}} \cong \frac{g(\{\tilde{x}\})_k - g(\{x\})_k}{h} \quad (3-53)$$

The gradients are determined for the objective function and all constraints with respect to all design variables of all panels to obtain a completely filled gradient matrix as indicated in Table 3-1 (without the objective function). The first index denotes the panel and the second the constraint respectively the design variable for example $g_{1,2}$ stands for constraint 2 of panel 1 and $x_{1,2}$ is the second design variable of panel 1.

The constraints bounding the feasible domain of the design variables of one panel are only dependant on the design variables of that relevant panel. Therefore the gradients with respect to design variables of other panels, positioned outside the diagonal of the gradient matrix, are zero. These gradients are denoted as local gradients. The constraints describing the failure criteria for strength and buckling of one panel are dependent on the design variables of the panel itself and on other panels. An example would be the impact of a laminate thickness change of panel 1 on the strength of panel 2. Such possible load re-

distributions between the panels are covered by the off-diagonal terms of the global gradient matrix which cannot be determined with analytical methods.

The last rows of the gradient matrix represent the gradients for the constraints on assembly level which means that these constraints are functions of a design variable of several panels for example linking the lamination parameter V_1^{*A} of panel 1 and 2. A more detailed description will be given in section 4.

Table 3-1: Matrix containing the gradients

		Panel 1			Panel 2			...	Panel m	
		$x_{1,1}$	$x_{1,2}$...	$x_{2,1}$	$x_{2,2}$	$x_{m,n}$
Panel 1	$g_{1,1}$	$\frac{dg_{1,1}}{dx_{1,1}}$	$\frac{dg_{1,1}}{dx_{1,2}}$...	$\frac{dg_{1,1}}{dx_{2,1}}$	$\frac{dg_{1,1}}{dx_{2,2}}$	$\frac{dg_{1,1}}{dx_{m,n}}$
	$g_{1,2}$	$\frac{dg_{1,2}}{dx_{1,1}}$	$\frac{dg_{1,2}}{dx_{1,2}}$...	$\frac{dg_{1,2}}{dx_{2,1}}$	$\frac{dg_{1,2}}{dx_{2,2}}$	$\frac{dg_{1,2}}{dx_{m,n}}$

Panel 2	$g_{2,1}$	$\frac{dg_{2,1}}{dx_{1,1}}$	$\frac{dg_{2,1}}{dx_{1,2}}$...	$\frac{dg_{2,1}}{dx_{2,1}}$	$\frac{dg_{2,1}}{dx_{2,2}}$	$\frac{dg_{2,1}}{dx_{m,n}}$
	$g_{2,2}$	$\frac{dg_{2,2}}{dx_{1,1}}$	$\frac{dg_{2,2}}{dx_{1,2}}$...	$\frac{dg_{2,2}}{dx_{2,1}}$	$\frac{dg_{2,2}}{dx_{2,2}}$	$\frac{dg_{2,2}}{dx_{m,n}}$

...
Panel m
	$g_{m,n}$	$\frac{dg_{m,n}}{dx_{1,1}}$	$\frac{dg_{m,n}}{dx_{1,2}}$...	$\frac{dg_{m,n}}{dx_{2,1}}$	$\frac{dg_{m,n}}{dx_{2,2}}$	$\frac{dg_{m,n}}{dx_{m,n}}$
Assembly 1	g_{A1}		$\frac{dg_{A1}}{dx_{1,2}}$...	$\frac{dg_{A1}}{dx_{2,1}}$		$\frac{dg_{A1}}{dx_{m,n}}$

...

3.5.3 Selection of the optimizer

The selection of the optimizer is based on the requirements that result from the optimization problem. The algorithm has to be able to process gradients of a linear objective function and non-linear inequality constraints. The non-linear inequality constraints result from the description of the feasible domain given in section 3.4. Furthermore the selected algorithm has to consider the definition of upper and lower bounds for the design variables namely the normalized lamination parameters whose design space is limited by -1 and 1 as described in section 3.4. Based on these requirements an algorithm is chosen out of the free available packages for the python environment. For the first implementation of the optimization algorithm in VErSO which constitutes the basis of the present work the MMA algorithm of NLOpt [27] is used. NLOpt is an open-source library for non-linear optimization that provides an interface to a number of different algorithms callable, inter alia, from Python.

MMA stands for “Method of Moving Asymptotes” and is based on the CCSA (Conservative Convex Separable Approximation) approach developed by Svanberg [28]. In each step a local and convex approximation in form of a sub-problem is generated. First the values for the constraints and the

gradients of the constraints are determined for the given iteration. Based on these values the usually implicit functions are replaced by approximating explicit functions. A quadratic penalty term is used to keep the approximating functions conservative (greater or equal) with respect to the exact functions.

The optimal solution of the sub-problem constitutes the possible candidate for the next design point. The objective and constraints are evaluated and in case that the approximating functions are conservative the iteration is completed and the process is restarted at the new design point. If that is not the case the penalty term of the approximations is increased and a new solution of the sub-problem is generated and checked for conservativeness.

3.5.4 Convergence criteria

There are several termination options available in NLOpt [27]. One option is the definition of an absolute or a relative tolerance based on the function values. The best way would be to set the error in relation to the optimum function value but this is not possible since the optimum is not known. To overcome this most algorithms consider the change of the function value between two consecutive iterations like formulated in the following equation:

$$\frac{|f^q - f^{q-1}|}{|f^q|} \leq f_{tol} \quad (3-54)$$

The same can be done based on the design variables. A further termination criterion is the definition of a stopping value. The algorithm stops when the objective function reaches the specified value for any feasible design point $\{x\}$.

In the most applications the relative tolerance criterion is used, which is also the case for the present work and the optimization process described in the following section. The advantage using a relative criterion is the independence of any units or scale factors. The tolerance value should be chosen in accordance with the machine precision. Close to the minimum the change of the function value based on the Taylor series expansion can be described with the following equation.

$$f(\{x^q\}) - f(\{x^{q-1}\}) \approx \frac{1}{2} f''(\{x^{q-1}\}) (\{x^q\} - \{x^{q-1}\})^2 \quad (3-55)$$

Assuming a variation in the design values of 10^{-6} would produce a change in the objective of 10^{-12} which leads to the assertion that a requested tolerance for the design values should be smaller than the square root of machine precision. Generally NLOpt terminates the process when the first (weakest) termination condition is fulfilled.

3.5.5 Optimization process

Before the optimization can be started the process needs to be initialized as shown in Figure 3-13. The necessary information can be taken out of any input file, here the FE-model is used. The model structure defines the hierarchical relation between assemblies, components and finite elements (from top level to bottom level) and is needed to initialize the object model. Component properties like the geometry are required to determine the buckling length. The material properties are used to set up the constraints for buckling and strength.

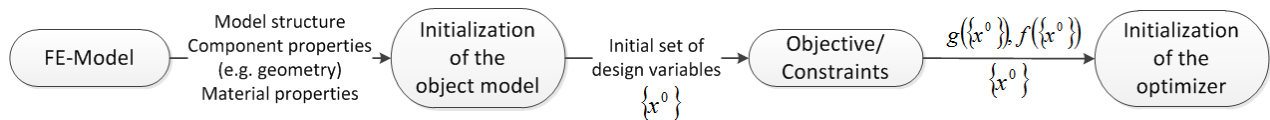


Figure 3-13: Initialization of the optimization

Based on the model structure the initialization of the object model is done on three levels. The initialized component objects are committed to the related assembly. All assemblies belong to one wing object. After the object model is created the design parameters have to be indexed. The structure of the object model and the procedure of indexing are shown in Figure 3-14 for an example with two assemblies, each having two components. Each component has two design parameters.

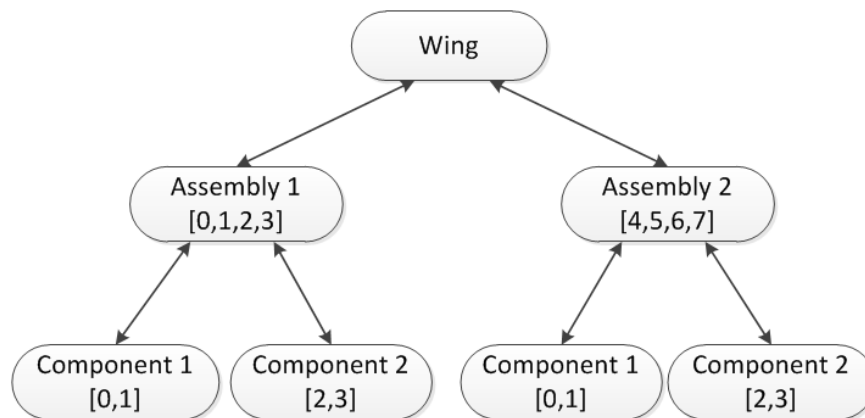


Figure 3-14: Object model structure and indexing of the design parameters

The indexing is done by a function on the wing level. It generates a set of indices by asking for the parameter sets of the design variables and constraints for every assembly and all related components. As shown in Figure 3-14 for assembly 2 the translation of indices is done between the component and assembly level. In case that a new design parameter set provided by the optimizer has to be assigned to the object model, the same strategy of index slicing is used. Every object on every level knows only its own parameters. This allows a formulation of constraints on component as well as on assembly level without knowing the complete structure of the wing. Once the object model is initialized, a set of start design variables is provided for which the objective and the constraints are evaluated. The complete parameter set is sent to the optimizer for his initialization.

Based on the initial parameter set the optimizer determines the first design parameter set. The running optimization process is sketched in a simplified way in Figure 3-15. It has to be noted that the sketch is focused on the process and not on the data flow. Not all passed data are used by the next function. The FE interface uses the new design parameter set to calculate the finite element loads and post-process

them to obtain the panel design loads based on the element peak method. This method determines the critical element load of a panel for a series of metrics. Using the strength metric as an example only the highest $+\hat{n}_x$ is taken as the design load.

With the panel loads $\{\hat{n}^{q+1}\}$ and the new design parameter set $\{x^{q+1}\}$, the constraint values are updated. Also the objective $f\{x^{q+1}\}$ is evaluated with the new parameter set. The set of constraints and objective is used by the optimizer to generate a new design parameter set for the next iteration. The process ends when one of the set convergence criteria (described in the previous section) is satisfied.

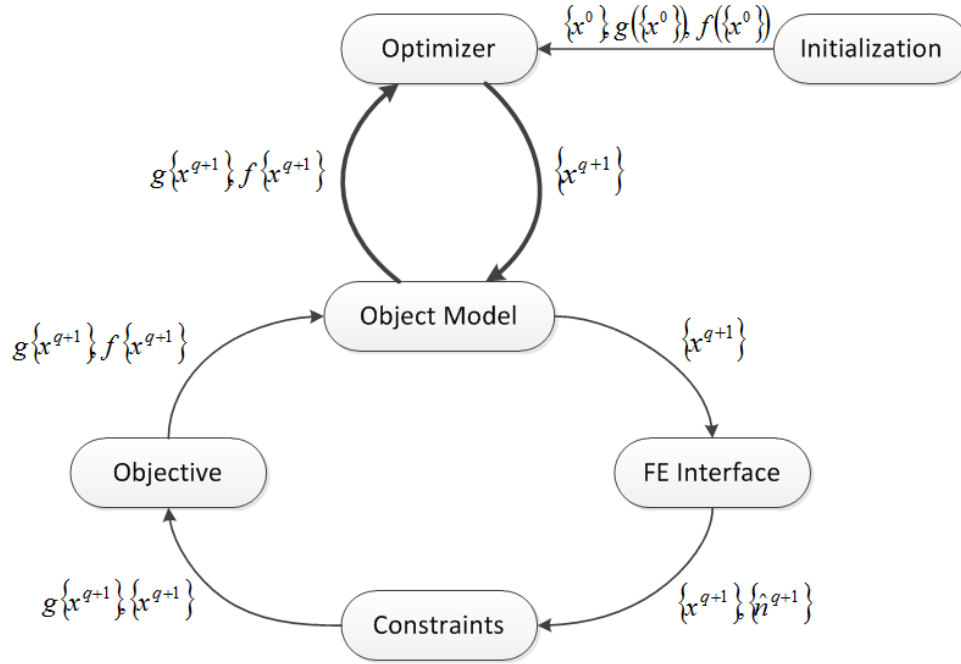


Figure 3-15: Running optimization process in VErSO

3.6 Conversion from LPs to a laminate configuration

For the final evaluation of the laminate configuration the optimal LP set of a panel found by the optimizer has to be transformed back to a discrete stacking sequence. Based on the discussion about the feasible domain of lamination parameters in section 3.4 it can be concluded that there is no closed form solution to convert any single design point in the LP space into a unique laminate stacking sequence. As shown in Figure 3-9 (left) the possible stacking sequences correspond to discrete design points in the LP space. Using the LPs as continuous design variables in an optimization procedure is not exact, because the closest LP set that describe a real stacking has to be chosen. This error gets smaller with an increasing number of plies and can be neglected in the preliminary stage of the design process.

Two special cases can occur when converting an optimal found LP set to a discrete laminate stacking. The first case is that several discrete design points representing real stackings are equally close to the optimal found LP set e.g. surround it. The second case is that the found LP set represents more than one stacking as described with Figure 3-8. Both cases have the advantage that more than one stacking is available for a panel. Therefore the stackings of two neighbouring panels can be chosen in a way that they best fulfill the selected design rules in longitudinal direction.

4. Implementation of design rules in the optimization algorithm

The previously described optimization process VErSO uses the four lamination parameters $V_{[1,2]}^{*A,D}$ as continuous design variables. The restriction on only 4 out of 12 LPs implies the two design rules in thickness direction namely the usage of only symmetric and balanced laminates as detailed discussed in section 3.2 and 3.4. Two types of constraints for the two individual panels are taken into account, the failure constraints and the constraints that restrict the LP space of each panel as described in section 3.4.

The goal of the present section is to formulate the selected design rules (see section 2.3) in longitudinal direction as assembly constraints to restrict the change in thickness and in the LPs between the two panels during the optimization.

The state of the art for existing formulations of the selected design rules as appraisable design criteria are documented in section 4.1. A modified design criterion that combines two of the existing formulations for the design rules “Taper slope” and “Continuity of plies” is presented in section 4.2. Based on this modified design criterion constraints are set up for the assembly of two adjacent laminates which is described in section 4.3. A comparison to an existing constraint formulation for the LP space is given in section 4.4 followed by the implementation of the assembly constraints in the optimization environment VErSO in section 4.5.

4.1 State of the art

The present section gives an introduction into existing formulations of the selected design rules as appraisable design criteria within an optimization process. Liu et al. [1] developed the so-called stacking sequence criterion that represents the ply continuity as a measure of continuous plies between two adjacent laminates (respectively two neighbouring optimization regions). A continuous ply occurs in both laminates and is separated in thickness direction by only one terminated ply. It does not matter whether the terminated ply is part of the thinner or thicker laminate. An example is given in Figure 4-1.

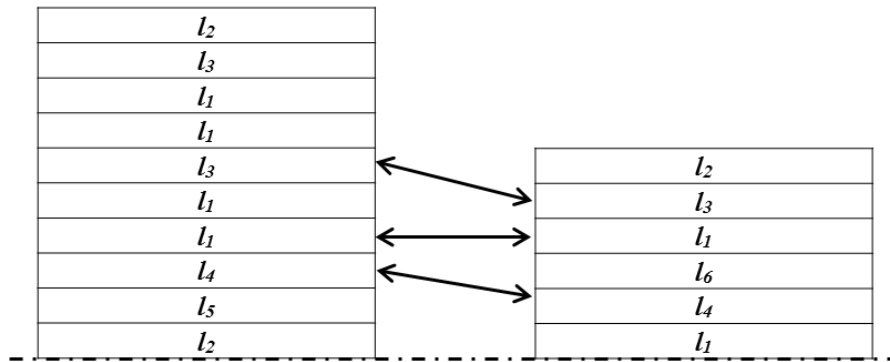


Figure 4-1: Stacking sequence continuity [1]

The outermost ply l_2 is not treated as continuous due to the separation of three truncated plies in-between. The thickness of continuous plies can be calculated with the following equation where $t(l_i)$ denotes the thickness of ply l_i .

$$t_{cont} = t(l_3) + t(l_1) + t(l_4) \quad (4-1)$$

The two-sided stacking sequence continuity C is determined by the following equation where T_1 denotes the total thickness of laminate 1 respectively T_2 the thickness of laminate 2.

$$C_{1 \rightarrow 2} = \frac{t_{cont}}{\max\{T_1, T_2\}} \quad (4-2)$$

A further method to obtain a certain degree of ply continuity and to follow a certain ply drop technique as described in section 2.1 is the so called laminate blending for which various definitions have been developed in the last years. In the blending definition of Adams [2], stacking sequences can only be blended outwardly (respectively inwardly) if the stacking of panel 1 is obtained by removing the outermost plies (respectively innermost). To obtain a globally blended design a genetic algorithm is used to find an optimal stacking guide for the complete structure. The stacking guide is used for the thickest panel and the stackings of all other panels of the structure are obtained by dropping plies of the stacking guide, as shown in Figure 4-2.

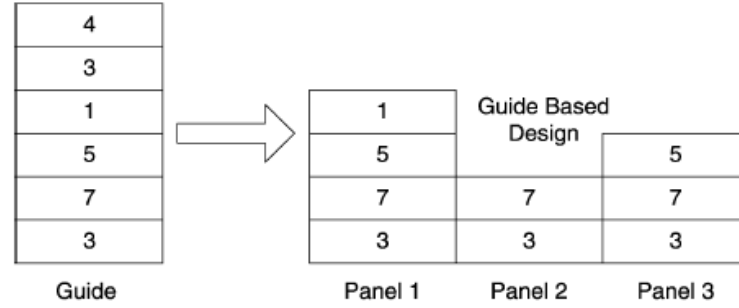


Figure 4-2: Guide based design completely outwardly blended [2]

The two approaches presented above are formulated for discrete stacking sequences and therefore in their originally form not usable for the optimization with the continuous LPs. In 2015 Macquart et al. [3] developed an approach that takes into account blending constraints for the LP space. Based on the author's knowledge this is the only available analytical method formulated for the LP space until today. He quantifies the change in lamination parameters (LPs) due to ply drops. Equation (4-3) shows the change in the LP V_1^A where X specifies any number of removed plies out of the set S and N denotes the total number of plies.

$$\begin{aligned} \Delta V_{1(N) \rightarrow (N-X)}^A &= \Delta V_{1(N)}^A - \Delta V_{1(N-X)}^A \\ &= \frac{1}{N} \sum_{\substack{j=1 \\ j \in S}}^X \cos(2\theta_j) + \left(\frac{1}{N} - \frac{1}{N-X} \right) \sum_{\substack{i=1 \\ j \notin S}}^N \cos(2\theta_i) \end{aligned} \quad (4-3)$$

From the equation above it can be derived that the maximal and minimal delta values occur for $[\theta_i; \theta_i] = [0^\circ; 90^\circ]$ and $[\theta_i; \theta_i] = [90^\circ; 0^\circ]$. Macquart numerically verified the above equation by generating three different pools of stacking sequences, one randomly generated, the second one with symmetric laminates of 0° , $\pm 45^\circ$ and 90° plies and the third one with extreme laminates. Extreme laminates in this context specify laminates in which all plies have the same orientation angle. Figure 4-3 shows the result for V_1^A and it can be observed that the maximum change in the LPs occur for extreme laminates. Therefore the complete constraint formulation of Marquardt is based on extreme laminates.

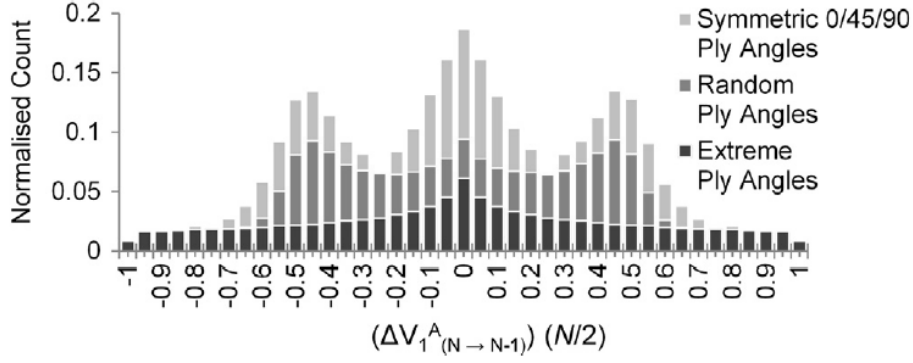


Figure 4-3: Normalised change in lamination parameter V1 due to one ply-drop [3]

Based on this restriction equation (4-3) can be simplified and generalized for the other in-plane LPs as follows:

$$\|\Delta V_{k(N) \rightarrow (N-X)}^A\| \leq 2 \left(\frac{X}{N} \right) \quad (4-4)$$

To consider the variation of two LPs at the same time Macquart uses the Euclidian distance to formulate the constraint. The maximum of the Euclidian distance can be associated with the allowable radius within the LP space referring to dropped plies. This radius reaches its maximum when using extreme laminates. Macquart calculated for all combinations of two LPs the factor $f_k(\theta_j, \theta_i)$. In case of $\Delta V_1^{A,D}$ and $\Delta V_2^{A,D}$ this factor is still 2. The generalized constraint formulation for in-plane LPs is given in equation (4-5) and for out-of-plane LPs in equation (4-6).

$$E_{k(N) \rightarrow (N-X)} \leq \sqrt{\max f_k(\theta_j, \theta_i)} \left(\frac{X}{N} \right) \quad (4-5)$$

$$E_{k(N) \rightarrow (N-2X)} \leq 2 \sqrt{\max f_k(\theta_j, \theta_i)} \left(3 \left(\frac{X}{N} \right) - 6 \left(\frac{X}{N} \right)^2 + 4 \left(\frac{X}{N} \right)^3 \right) \quad (4-6)$$

The above constraint formulation guarantees that no blended solution exists in case that the constraint is not fulfilled. The formulation is very conservative because the factor 2 covers in general the complete lamination parameter space. The constraint is mainly driven by the taper ratio X/N . Another critical point is that the usage of only extreme laminates is generally avoided due to design rules as specified in section 2.1 and 2.2. Furthermore it must be questioned if the application of laminate blending (e.g. usage of a stacking guide) is still sensible when using only extreme laminates which are blended in any case. The advantages with respect to manufacturability of blended laminates should not be cancelled out by the disadvantages of extreme laminates and their restricted structural performance.

The two presented design criteria from Liu et al. [1] and Adams et al. [2] are formulated for discrete stacking sequences and therefore in their original form not usable for the optimization with continuous LPs. The constraint formulation of Macquart et al. [3] for the LP space and blended laminates seems to be too conservative as will be shown in section 4.4.

The goal is to formulate a modified design criterion for the LP space that allows the combination of the design rules selected in 2.3. This criterion is based on the approaches from Liu et al. [1] and Adams et al. [2]. It is used in section 4.3 to derive constraints that restrict the LP space for the gradient-based optimization process VErSO described in section 3.6.

4.2 A modified design criterion

A modified design criterion that combines the requirements regarding ply continuity and a specified taper slope for terminating plies can be formulated on the basis of the described approaches from Liu et al. [1] and Adams et al. [2]. The blending concept is adopted but in a generalised way. All plies of the thinner laminate have to be existent in the thicker one to fulfill the blending but they do not have to be inwardly or outwardly blended.

According to the design rule “Taper slope and maximum thickness step” the overall maximum thickness step between two adjacent laminates is limited to 0.508mm (4 plies) in principal. To keep the computational costs manageable the detailed tapering of terminated plies along the longitudinal direction cannot be considered within the optimization. The tapering areas have to be summarized to discrete thickness changes at the borders between two optimization regions as shown in Figure 4-4. Therefore a restriction in the maximum thickness step at one interface is not helpful and instead of a taper slope the taper ratio defined as number of removed plies over all plies is used.

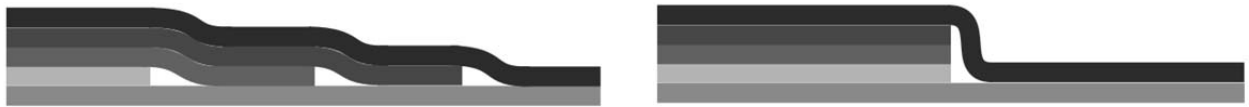


Figure 4-4: Tapering areas based on a taper slope (left) summarized to a discrete thickness step (right)

For applications of larger structures with more than two optimization regions the taper ratio between two adjacent panels should be automatically determined based on their geometrical size. This implies that for larger optimization regions a higher taper ratio (thickness step) should be allowed to cover all terminated plies of the section in longitudinal direction that belongs to the respective optimization region. During the real manufacturing process the thickness change can be splitted into two or more thickness steps to get a smoother transition. For the present application of two optimization regions the taper ratio is used as percentage of the terminated plies with respect to the thicker laminate in the following.

The position of the terminating plies is generally driven by the continuity criterion of Liu et al. [1]. Following the criterion strictly would lead to the fact that mainly all terminated plies are located outwardly like shown in Figure 4-5 for a blended laminate of 12 plies, 50% ply continuity and a taper ratio of 50%. There are two reasons for that behaviour. First the restrictive definition of a continuous ply (step of only one ply in thickness is allowed) leads to the fact that only one terminated ply can be located inwardly or between the continuous plies and all other terminated plies have to be located outwardly above the continuous plies. Furthermore it has to be noted that the allowable step in thickness direction of one ply is referred to the mid-plane.

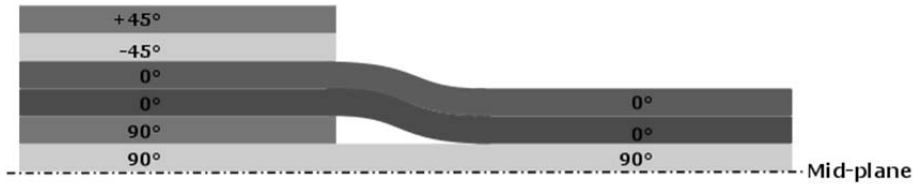


Figure 4-5: Blended laminate with 12 plies, 50% ply continuity and 50% taper ratio

The ply continuity definition of Liu et al. [1] is evaluated as too restrictive. Therefore the allowable step in thickness direction of a continuous ply is set to four plies. For other applications with more than two optimization regions, this value should also be adapted based on the panel size like already mentioned for the taper ratio. In contrast to the definition of Liu the allowable thickness step is not referred to the mid-plane but to the undermost ply. For a real manufacturing of a composite structure a continuous outer skin is required. Generally negative moulding tools are used and therefore the outermost ply is the ply which is placed at first and the stacking is build-up inwardly. One possible blended laminate based on the new continuity definition is shown in Figure 4-6. It has to be noted that the reachable ply continuity is limited by the taper ratio ($\text{ply continuity} \leq 1 - \text{taperRatio}$). It can be observed that the same plies are continuous as in Figure 4-5. The difference is that four terminated plies are located inwardly, because the allowable step of a continuous ply in thickness direction is selected to 4 plies.

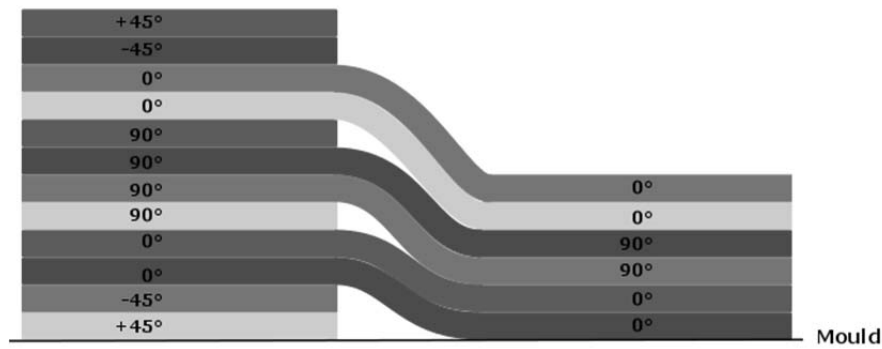


Figure 4-6: Blended laminate with 50% ply continuity and 50% taper ratio, new definition of continuous plies

A modified design criterion that combines the two design rules regarding the ply continuity and a prescribed taper ratio could be formulated. The mathematical formulation of this design criterion as constraint is given in the following section.

4.3 Assembly constraints formulation

In the present section the previously formulated design criterion is applied on discrete stackings to evaluate the influence of the design rules on the lamination parameter. Based on that results, equations shall be derived that interrelate the LPs of adjacent panels and restrict their feasible domain.

4.3.1 Approach

To evaluate the influence of the design rules on the lamination parameter a parameter study is carried out in the programming language Python. A material is selected and it is assumed that all plies of the laminates have the same material. The material data are given in section 5.1. The process of the parameter study can be structured in the following three steps for one selected laminate thickness (respectively number of plies). The first step is to generate all possible stackings that fulfill the design

criterion in thickness direction namely the usage of only symmetric and balanced laminates. It is assumed that the mid-plane of a symmetric laminate is located between two plies. For every generated stacking all reduced stackings that fulfill the design criterion are determined within the second step. The reduced stackings have to fulfill the design criterion in thickness direction as well as in longitudinal direction which includes the taper ratio, the blending and the ply continuity. As described in the previous section the taper ratio is treated as percentage of the terminated plies with respect to the thicker laminate. In the third step the differences of the LP sets $\Delta V_{[1,2]}^{*A,D}$ between every reduced and the original stacking are calculated. The process is illustrated in Table 4-1 for a symmetric and balanced laminate of 12 plies. The allowable number of removed plies is 4. Every reduced stacking represents a feasible point in the domain of the LPs $\Delta V_{[1,2]}^{*A,D}$.

Table 4-1: Exemplary process to obtain the changes in LPs for the reduced stackings of one original stacking

Original Stacking	Reduced Stacking	ΔV_1^A	ΔV_2^A	ΔV_1^D	ΔV_2^D
$[45,-45,0,0,90,90]_s$	$[45,-45,0,0]_s$	0.5	0.3	0.1	0.1
	$[45,-45,90,90]_s$	0.2	0.2	0.4	0.1
	$[45,-45,0,90]_s$	0.2	0.4	0.2	0.2
	$[0,0,90,90]_s$	0.3	0.2	0.4	0.8
$[45,-45,90,0,0,90]_s$	$[45,-45,0,0]_s$	0.5	0.3	0.1	0.1
	$[45,-45,90,0]_s$	0.2	0.45	0.2	0.2

...

4.3.2 Mathematical formulation

Based on all feasible points two different mathematical approaches are investigated. In the first approach the maximum change of every LP over all reduced stackings is determined. Every maximum change of one LP could be produced by a different reduced stacking as marked with orange colour in Table 4-1. Furthermore it can be observed that for different original stackings the same reduced stacking can be obtained. Only the LP sets (rows in Table 4-1) where a maximum value occur in one of the four columns $\Delta V_{[1,2]}^{*A,D}$ are taken as points to construct the convex feasible domain as shown later.

The second approach is based on the calculation of a convex hull. As already shown in section 3.4 the LP space is convex and therefore also the difference values form a convex set. A Python interface of the QHULL function developed by Barber [29] is used to calculate the convex hull of all points. Each point (one row in Table 4-1) in a four-dimensional space is represented by the four values $\Delta V_{[1,2]}^{*A,D}$. Equation (4-7) is used to determine the convex hull with X denoting the finite set of points.

$$C_H(X) = \left\{ \sum_{i=1}^N \lambda_i X_i \mid \lambda_i \geq 0, \quad i = 1, \dots, N, \quad \sum_{i=1}^N \lambda_i = 1 \right\} \quad (4-7)$$

As shown in Figure 4-7 the convex hull of the delta values results in a convex polyhedron formed by the minimum number of points on the boundary of the feasible domain. Furthermore it can be observed that the polyhedron is bounded by a set of hyperplanes. The QHULL function of Barber et al. [29] outputs a set of vertices for each hyperplane. In the present case of a four-dimensional space, four vertices are

necessary to describe a hyperplane. Based on the set of vertices the five coefficients for each hyperplane can be determined with equation (4-8).

$$\begin{aligned}
 h_1 &= \det \begin{pmatrix} 1 & \Delta V_{2,1}^{*A} & \Delta V_{1,1}^{*D} & \Delta V_{2,1}^{*D} \\ 1 & \Delta V_{2,2}^{*A} & \Delta V_{1,2}^{*D} & \Delta V_{2,2}^{*D} \\ 1 & \Delta V_{2,3}^{*A} & \Delta V_{1,3}^{*D} & \Delta V_{2,3}^{*D} \\ 1 & \Delta V_{2,4}^{*A} & \Delta V_{1,4}^{*D} & \Delta V_{2,4}^{*D} \end{pmatrix} & h_2 &= \det \begin{pmatrix} \Delta V_{1,1}^{*A} & 1 & \Delta V_{1,1}^{*D} & \Delta V_{2,1}^{*D} \\ \Delta V_{1,2}^{*A} & 1 & \Delta V_{1,2}^{*D} & \Delta V_{2,2}^{*D} \\ \Delta V_{1,3}^{*A} & 1 & \Delta V_{1,3}^{*D} & \Delta V_{2,3}^{*D} \\ \Delta V_{1,4}^{*A} & 1 & \Delta V_{1,4}^{*D} & \Delta V_{2,4}^{*D} \end{pmatrix} \\
 h_3 &= \det \begin{pmatrix} \Delta V_{1,1}^{*A} & \Delta V_{2,1}^{*A} & 1 & \Delta V_{2,1}^{*D} \\ \Delta V_{1,2}^{*A} & \Delta V_{2,2}^{*A} & 1 & \Delta V_{2,2}^{*D} \\ \Delta V_{1,3}^{*A} & \Delta V_{2,3}^{*A} & 1 & \Delta V_{2,3}^{*D} \\ \Delta V_{1,4}^{*A} & \Delta V_{2,4}^{*A} & 1 & \Delta V_{2,4}^{*D} \end{pmatrix} & h_4 &= \det \begin{pmatrix} \Delta V_{1,1}^{*A} & \Delta V_{2,1}^{*A} & \Delta V_{1,1}^{*D} & 1 \\ \Delta V_{1,2}^{*A} & \Delta V_{2,2}^{*A} & \Delta V_{1,2}^{*D} & 1 \\ \Delta V_{1,3}^{*A} & \Delta V_{2,3}^{*A} & \Delta V_{1,3}^{*D} & 1 \\ \Delta V_{1,4}^{*A} & \Delta V_{2,4}^{*A} & \Delta V_{1,4}^{*D} & 1 \end{pmatrix} \\
 h_5 &= -\det \begin{pmatrix} \Delta V_{1,1}^{*A} & \Delta V_{2,1}^{*A} & \Delta V_{1,1}^{*D} & \Delta V_{2,1}^{*D} \\ \Delta V_{1,2}^{*A} & \Delta V_{2,2}^{*A} & \Delta V_{1,2}^{*D} & \Delta V_{2,2}^{*D} \\ \Delta V_{1,3}^{*A} & \Delta V_{2,3}^{*A} & \Delta V_{1,3}^{*D} & \Delta V_{2,3}^{*D} \\ \Delta V_{1,4}^{*A} & \Delta V_{2,4}^{*A} & \Delta V_{1,4}^{*D} & \Delta V_{2,4}^{*D} \end{pmatrix}
 \end{aligned} \tag{4-8}$$

Any point with the delta values $\Delta V_{[1,2]}^{*A,D}$ is located within the convex hull when equation (4-9) is fulfilled for every hyperplane forming the convex hull. This equation constitutes the main part of the constraint formulation.

$$h_1 \Delta V_1^{*A} + h_2 \Delta V_2^{*A} + h_3 \Delta V_1^{*D} + h_4 \Delta V_2^{*D} + h_5 \leq 0 \tag{4-9}$$

Figure 4-7 shows the comparison between the two approaches discussed above. It can be observed that the feasible domain constructed by the envelope of the $\Delta V_{[1,2]}^{*A,D}$ max. values (marked red) is significantly smaller in comparison to the convex hull of all feasible points (marked green). In case that each of the max. value would be treated constant over the other LPs the feasible domain would have the shape of a rectangular box and would be much larger than the feasible domain of the convex hull. Due to the large differences in the shape and size of the feasible domain, the first approach of constructing the feasible domain based on the $\Delta V_{[1,2]}^{*A,D}$ max. values is not suitable.

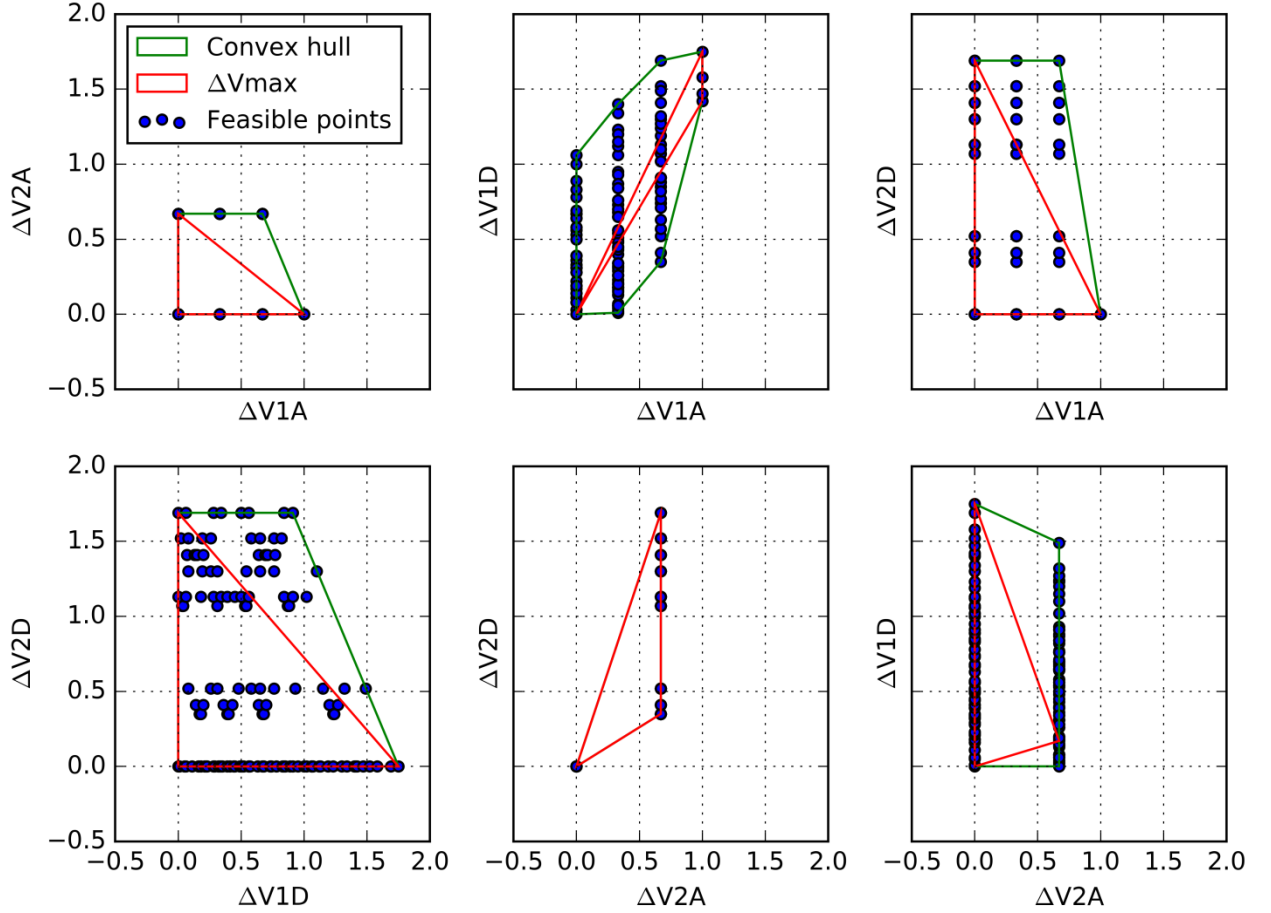


Figure 4-7: Comparison between the envelope of the ΔV_{\max} values and the convex hull for a laminate configuration with 12 plies a taper ratio of 0.5 and a required ply continuity of 0.5

The approach of constructing the feasible domain based on the convex hull is used for the constraint formulation (see equation (4-7)) and implementation in the optimization process. Thereby the convex hull serve as a measure for the compliance of the selected design rules.

4.3.3 Results of the parameter study

Based on the selected approach of the convex hull function, important results of the parameter study will be discussed to present the influence of the selected design rules on the feasible domain of the LP space. Figure 4-8 shows the number of hyperplanes and the volume size as characteristic properties of the convex hull depending on the number of plies. Between 10 and 18 plies the number of hyperplanes increases while the volume size decreases. It has to be noted that the number of removed plies stays constant within this range. A continuous value of the taper ratio 0.2 has to be converted to an even integer number of removed plies. 0.2 of 18 plies is 3.6 which has to be rounded down to 2 removable plies. The same happens in the range between 20 and 28 plies. Therefore the taper ratio has to be corrected for each laminate thickness individually. In case of 28 plies the number of removed plies is 4 and the corrected taper ratio is 0.14 instead of 0.2. Between 18 and 20 plies a doubling of the volume size can be observed. The optimization process described in section 3.5 works with a continuous thickness. To formulate the constraint a relation between the hyperplane coefficients and the laminate thickness has to be found. Due to the fact that the number of hyperplanes increases with the number of plies, a continuous dependence of the hyperplane coefficients on the laminate thickness is not given and an approximation e.g. with polynomial functions is not possible. Therefore a conservative approach is chosen

in which the next higher thickness value that represents an even integer number of plies is used. More details about the constraint implementation are given in section 4.5.

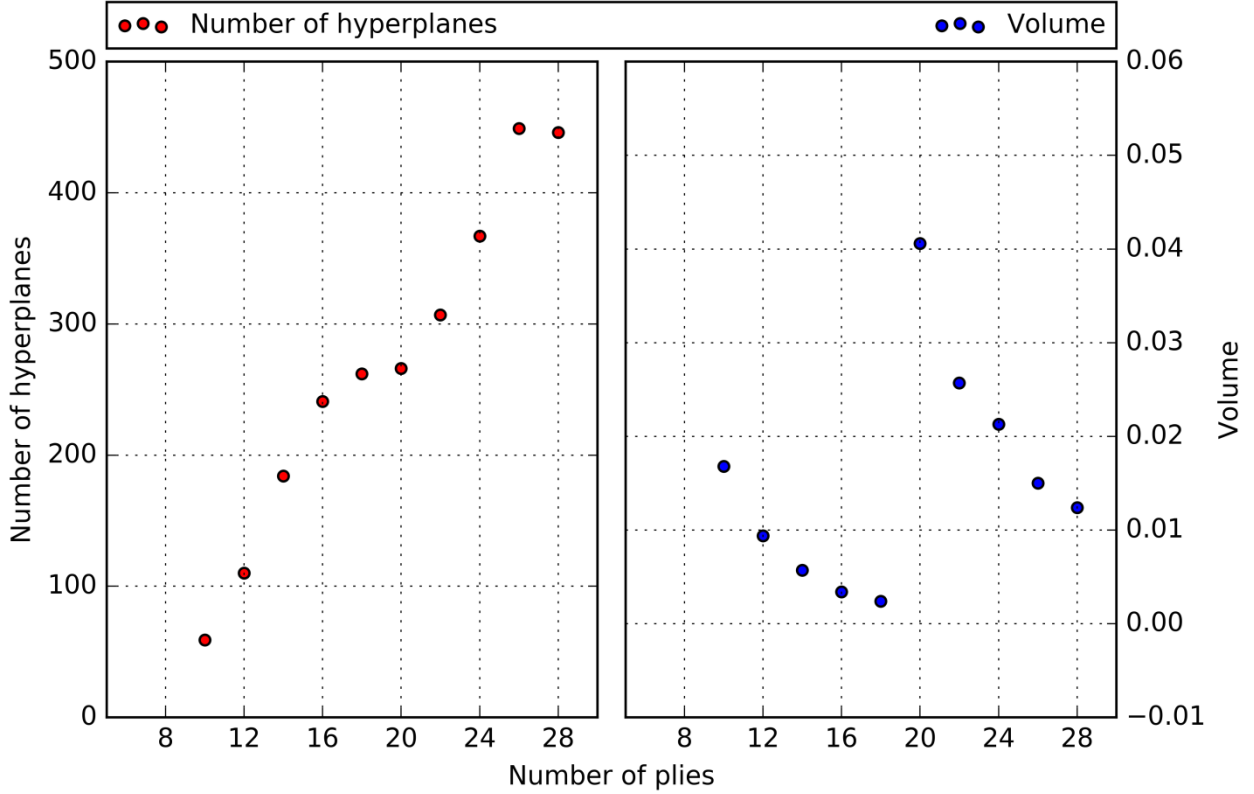


Figure 4-8: Number of hyperplanes and volume size over laminate thickness

The feasible domain of the four delta values $\Delta V_{[1,2]}^{*A,D}$ is shown in form of two-dimensional sectional views called subdomains in Figure 4-9, where the laminates consist of 12, 16 and 20 plies. The taper ratio is set to 0.2 and the ply continuity is 0.6. One effect can already be seen in the left column of Figure 4-7 comparing the subdomains $\Delta V_2^{*A} = f(\Delta V_1^{*A})$ and $\Delta V_2^{*D} = f(\Delta V_1^{*D})$. A higher scattering of the feasible points can be observed in the domain $\Delta V_2^{*D} = f(\Delta V_1^{*D})$. Every point in this domain represents one stacking sequence, whereas the LPs $\Delta V_{[1,2]}^{*A,D}$ representing the $[A]$ -matrix are independent of the stacking sequence, which leads to a significant smaller number of feasible points. Figure 4-9 shows that the shape of the feasible domain between 12 and 16 plies does not change significantly only the size decreases. Comparing the domains of 12 and 20 plies a change in the shape as well as an increase of the size is visible especially in the domain $\Delta V_2^{*D} = f(\Delta V_1^{*D})$. The increase of the size was already indicated in Figure 4-8 in form of a step between 18 and 20 plies. The reason for that is the conversion of the taper ratio as a continuous value to an even integer number of plies that can be removed. The general trend of the increasing number of hyperplanes as indicated in Figure 4-8 leads to a finer discretization of the feasible domain's boundary which can be seen when comparing the subdomains $\Delta V_1^{*D} = f(\Delta V_1^{*A})$ or $\Delta V_2^{*D} = f(\Delta V_2^{*A})$ for 12 plies and 20 plies (see Figure 4-9).

A comparison of Figure 4-7 and Figure 4-9 shows the change of the feasible domain when varying the design criterion for the taper ratio from 0.5 to 0.2. A completely different shape and a significantly smaller size in all subdomains can be observed.

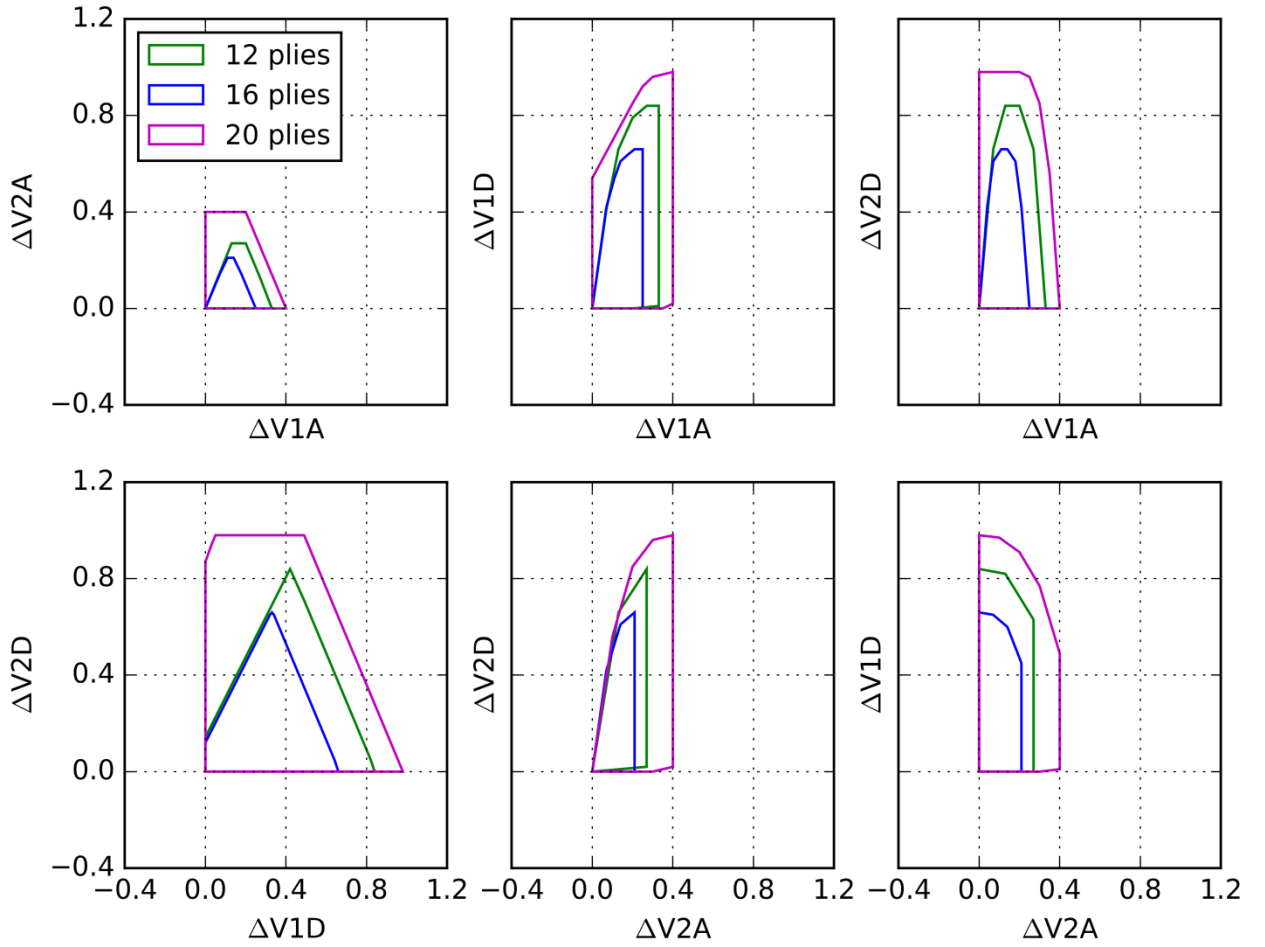


Figure 4-9: Feasible domains for 12, 16 and 20 plies with a taper ratio of 0.2 and a required ply continuity of 0.6

Reducing the ply continuity from 0.5 in Figure 4-7 to 0.0 in Figure 4-10 increases only the size of the subdomains $\Delta V_1^{*D} = f(\Delta V_1^{*A})$ and $\Delta V_2^{*D} = f(\Delta V_2^{*A})$. Neglecting the ply continuity leads to a higher number of allowable reduced stackings which increases the number of feasible points in the domain which can be seen when comparing Figure 4-7 and Figure 4-10.

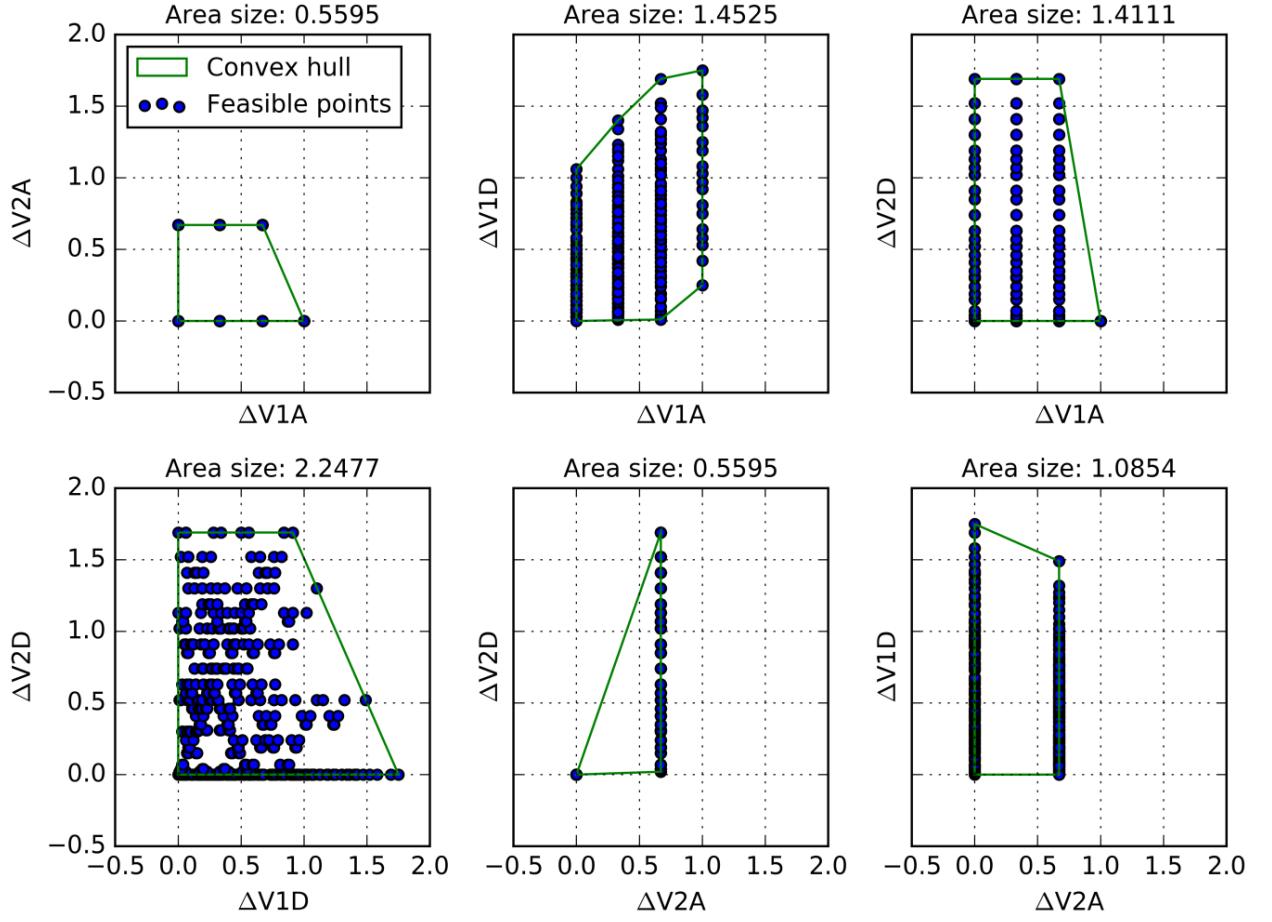


Figure 4-10: Feasible domain for 12 plies with a taper ratio of 0.5 and a required ply continuity of 0.0

4.4 Comparison to Macquart's constraints

The selected approach (see section 4.3) for constructing the feasible domain based on the convex hull should be compared to the method of Macquart et al. [3] already discussed in section 4.1. Macquart's construction of the feasible domain for $\Delta V_2^{*A} = f(\Delta V_1^{*A})$ and $\Delta V_2^{*D} = f(\Delta V_1^{*D})$ is based on the Euclidian distance as formulated in equations (4-5) and (4-6). Figure 4-11 shows that the feasible domain of Macquart's approach is significantly larger than the one generated by the convex hull especially for the domain $\Delta V_2^{*D} = f(\Delta V_1^{*D})$.

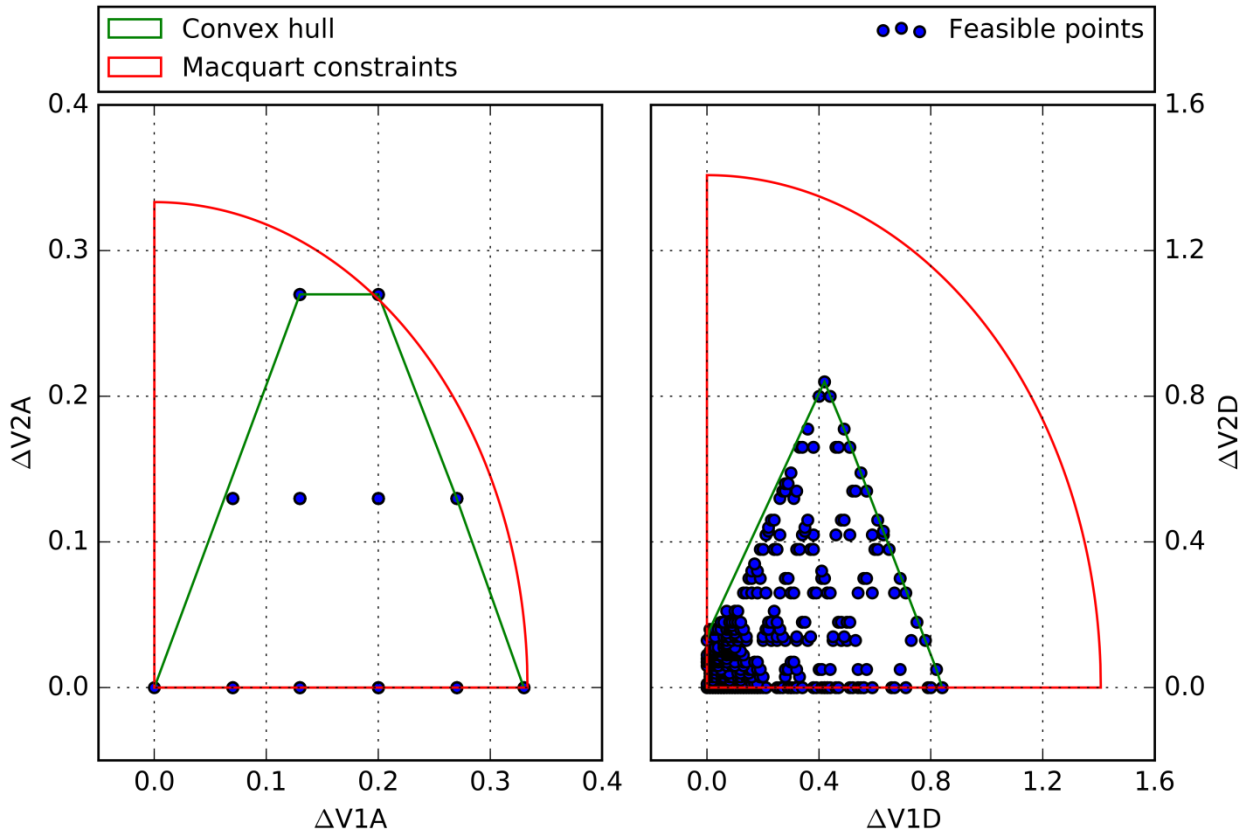


Figure 4-11: Comparison between Macquart's feasible domain and the convex hull for a laminate configuration with 12 plies a taper ratio of 0.2 and a required ply continuity of 0.6

A main advantage of Macquart's constraints is the usage of analytical equations that can be quickly evaluated by the optimizer. In addition, the constraint equations are independent from the material properties.

The determination of the hyperplane coefficients that describe the convex hull is much more computational-intensive and has to be done for all possible number of plies. The advantage is that the computation can be parallelized and distributed on several CPU's. The complete process of computing the constraints is done in advance of the optimization. The actual evaluation of the high number of linear constraint equations (see (4-9)) is quickly done by the optimizer.

4.5 Assembly constraints implementation

The present section describes the implementation of the assembly constraints based on the mathematical formulations given in section 4.3. Two assembly constraints are implemented, one for the taper ratio and a second one to represent the feasible change of the LP space for the two adjacent panels. The necessary input for the constraints are the design parameters namely the thickness values and the LP sets of both panels of the current iteration as shown in Figure 3-15.

The first assembly constraint imposes the allowable difference of the thickness between the two adjacent panels. The taper ratio is defined as percentage of the terminated plies with respect to the thicker laminate which has to be identified first. It has to be noted that the corrected taper ratio is used as explained in section 4.3.3. As an example for a laminate with 12 plies and an allowed taper ratio of 0.2 the number of removed plies is 2 and the corrected taper ratio therefore 0.167.

The constraint value which has to be equal or smaller than zero can be calculated with the following equation where $t_{2,Thin}$ specifies the thickness of the thinner panel 2.

$$\frac{(t_{2,Thin} - t_{1,Thick})}{t_{1,Thick}} - taperRatio \leq 0 \quad (4-10)$$

The second assembly constraint represents the feasible domain of the $\Delta V_{[1,2]}^{*A,D}$ values of the adjacent panels. Based on the approach given in section 4.3 the hyperplane coefficients representing a hyperplane of the convex hull are determined for all even numbers of plies between 10 and 30 and the material selected in section 5.1. The values are stored in a hierarchical data format (HDF) that links the data to the corresponding laminate thickness. As already explained in section 4.3.3 a continuous approximation of the hyperplane coefficients in dependent on the laminate thickness is not possible. To stay conservative the next higher thickness value that represents an even integer number of plies is used. Based on the constraint equation (4-11) the values for all hyperplanes are calculated. h_1 to h_5 denote the hyperplane coefficients and $\Delta V_{[1,2]}^{*A,D}$ the current LP set. The maximum value over all hyperplanes is taken as the constraint value and returned to the optimizer.

$$h_1 \Delta V_1^{*A} + h_2 \Delta V_2^{*A} + h_3 \Delta V_1^{*D} + h_4 \Delta V_2^{*D} + h_5 \leq 0 \quad (4-11)$$

5. Application of an example

An assembly of two components serves as an application example. The characteristic quantities of the optimization process VErSO are the structural mass as objective, the lamination parameters as design variables and three types of constraints. The failure constraints as well as the constraints that describe the LP space are present. Additionally the assembly constraints derived in section 4.3 are applied.

The FE-model described in section 5.1 is deliberately built up in a way that different load conditions occur in the two panels. The goal is to obtain more divergent design parameter sets (thickness and the LP set) of the two panels to evaluate in a second step how the assembly constraints prevent such a behaviour. The reference results of the optimized panels without assembly constraints are shown in section 5.2. The results including the assembly constraints are discussed in section 5.3.

5.1 Model and material definition

The FE-model is created with the software ANSYS [30]. The model consists of linear 4-node shell 181 elements as shown in Figure 5-1. The global y-axis is aligned with the panel length b in longitudinal direction. At $y = 0$ the compression load P_C acts with 15 N/mm on panel 1. The tension load P_T acts on the edge nodes at $y = 2b$ of panel 2 with 120 N/mm. A fixed bearing is applied to the nodes at $y = b$. The two nodes at $x = 0.5a$ and $y = 0; 2b$ are mounted by non-locating bearings (fixation in x- and z-direction). Furthermore the rotational degrees of freedom around y and z are suppressed.

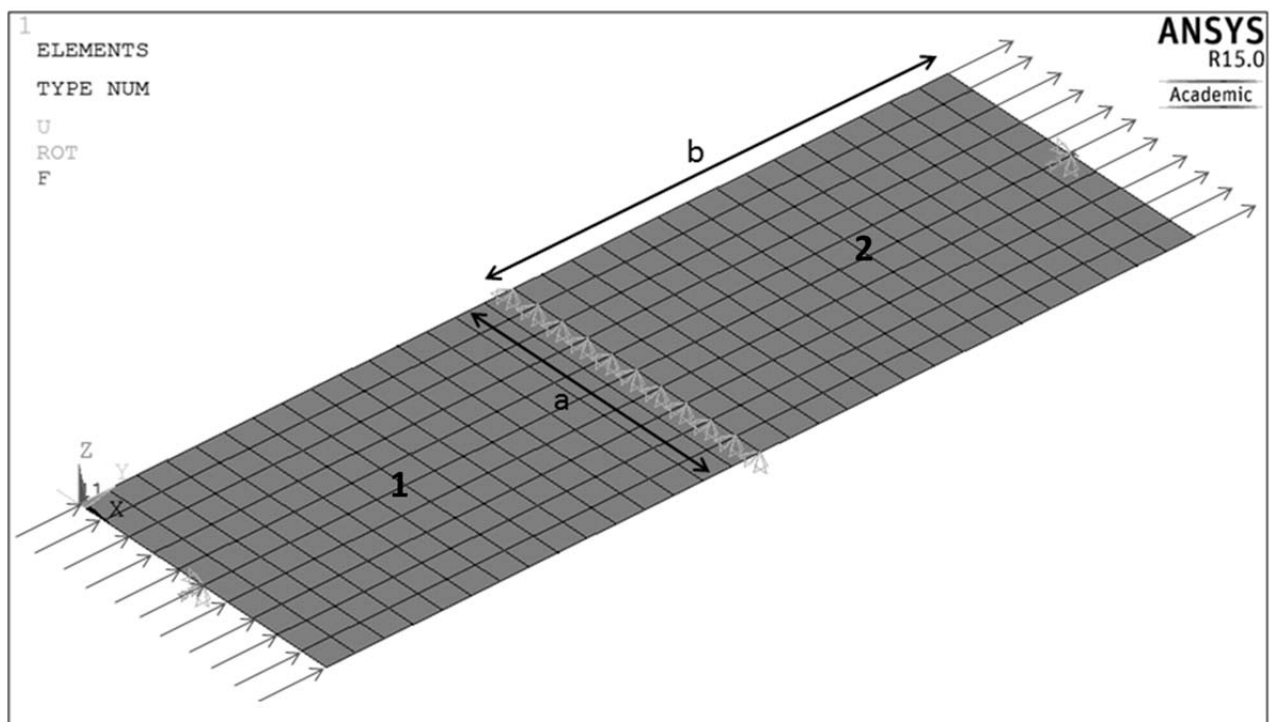


Figure 5-1: FE-model

The model data is shown in Table 5-1. The selected material is a Hexcel prereg T800/M21 [31]. Its data is listed in Table 5-2.

Table 5-1: Model data

Property	Value	Unit	Description
a	1000	mm	Width of both panels
b	1500	mm	Length in longitudinal direction of each panel
P_C	15	N/mm	Compression load of panel 1
P_T	120	N/mm	Tension load of panel 2

Table 5-2: Material data

Property	Value	Unit	Description
t_0	0.184	mm	Ply thickness
E_{11}	134.7	GPa	Young's modulus
$E_{22} = E_{66}$	7.7	GPa	
$\nu_{12} = \nu_{13}$	0.369		Poisson's ratio
ν_{23}	0.5		
$G_{12} = G_{13}$	4.2	GPa	Shear modulus
G_{23}	2.5	GPa	
ρ	0.1590	g/mm ³	Density
X_T	2290.5	MPa	Longitudinal tensile strength
X_C	1051	MPa	Longitudinal compression strength
Y_T	41.43	MPa	Transverse tensile strength
Y_C	210	MPa	Transverse compression strength
S_L	106.48	MPa	Shear strength

5.2 Reference results

The present section documents the reference results of the optimized two component model defined in the previous section without assembly constraints. Several starting parameters have been tested and the same optimization results could be achieved. The starting parameters given in Table 5-3 have been shown to be robust in terms of the convergence behaviour.

Table 5-3: Starting parameters of the optimizer

Parameter	Panel 1	Panel 2	Unit	Description
$V_{1,2}^{*A,D}$	0.1	0.1		Lamination parameters
T	2.5	2.5	mm	Panel thickness

It is expected that the minimum thickness of panel 1 under compressive load is driven by the failure criterion for compression buckling. For a resistance against buckling a higher proportion of $\pm 45^\circ$ plies is required. The corresponding extreme point in the LP domain $V_2^{*D} = f(V_1^{*D})$ would be $\{0; -1\}$ as shown in Figure 3-7. The minimum thickness of panel 2 under tension load should be driven by the failure criterion for strength which causes a higher proportion of 0° plies. The corresponding extreme point in the LP domain $V_2^{*A} = f(V_1^{*A})$ would be $\{1; 1\}$ as shown in Figure 3-7.

The results of the optimized panels without assembly constraints are shown in Table 5-4. It can be seen that the expected constraints of the particular panel are active.

Table 5-4: Results of the individually optimized panels

Result	Panel 1	Panel 2	Difference
V_1^{*A}	0.21	0.85	0.64
V_2^{*A}	-0.59	1.00	1.59
V_1^{*D}	0.01	0.64	0.63
V_2^{*D}	-0.98	1.00	1.98
$T [mm]$	4.00	1.99	2.01
Active failure constraint	Compression buckling	Strength	
Structural mass [kg]	14.29		

The mentioned extreme points have not been fully met as shown in Figure 5-2. The reason for that is an obstruction of the transverse contraction caused by the transition from tension to compression stresses. The resulting deformations in meters are shown in Figure 5-3 for longitudinal (left) and transversal direction (right).

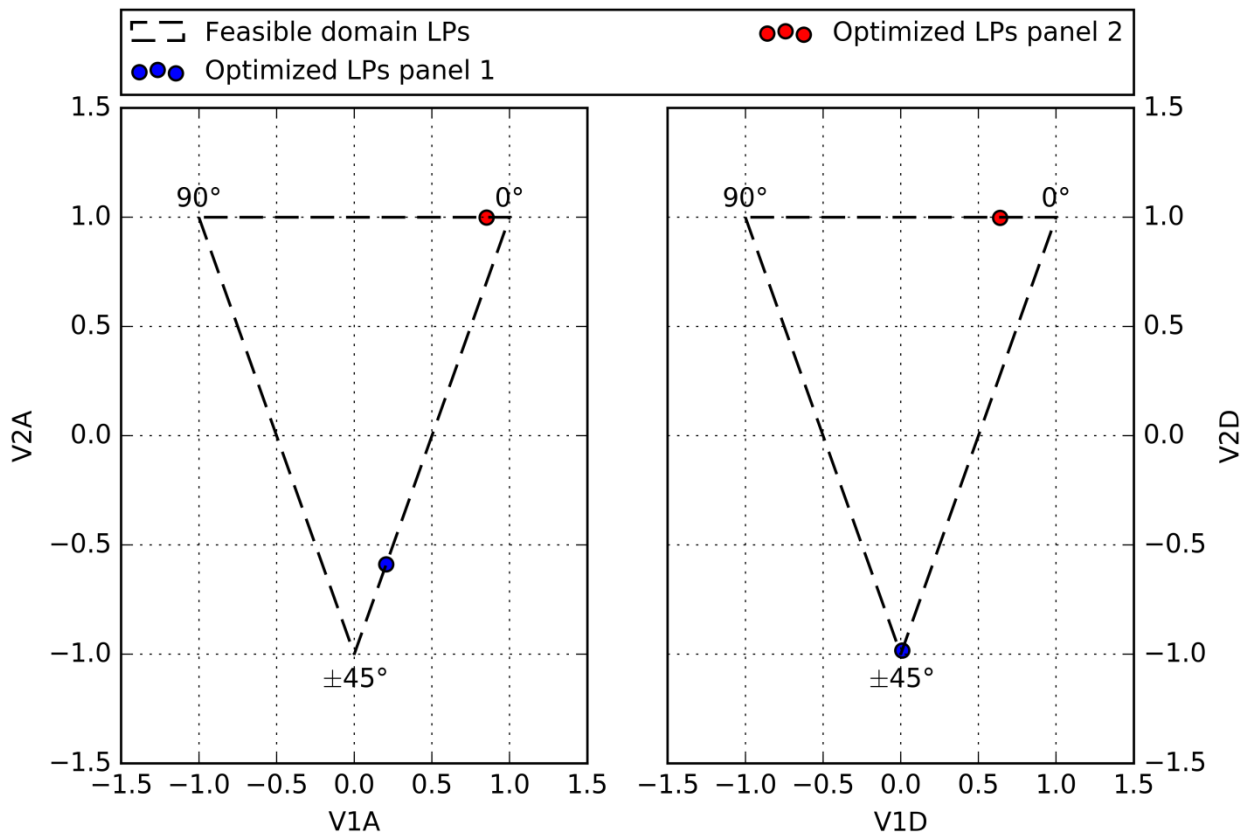


Figure 5-2: LP set of the individually optimized panels

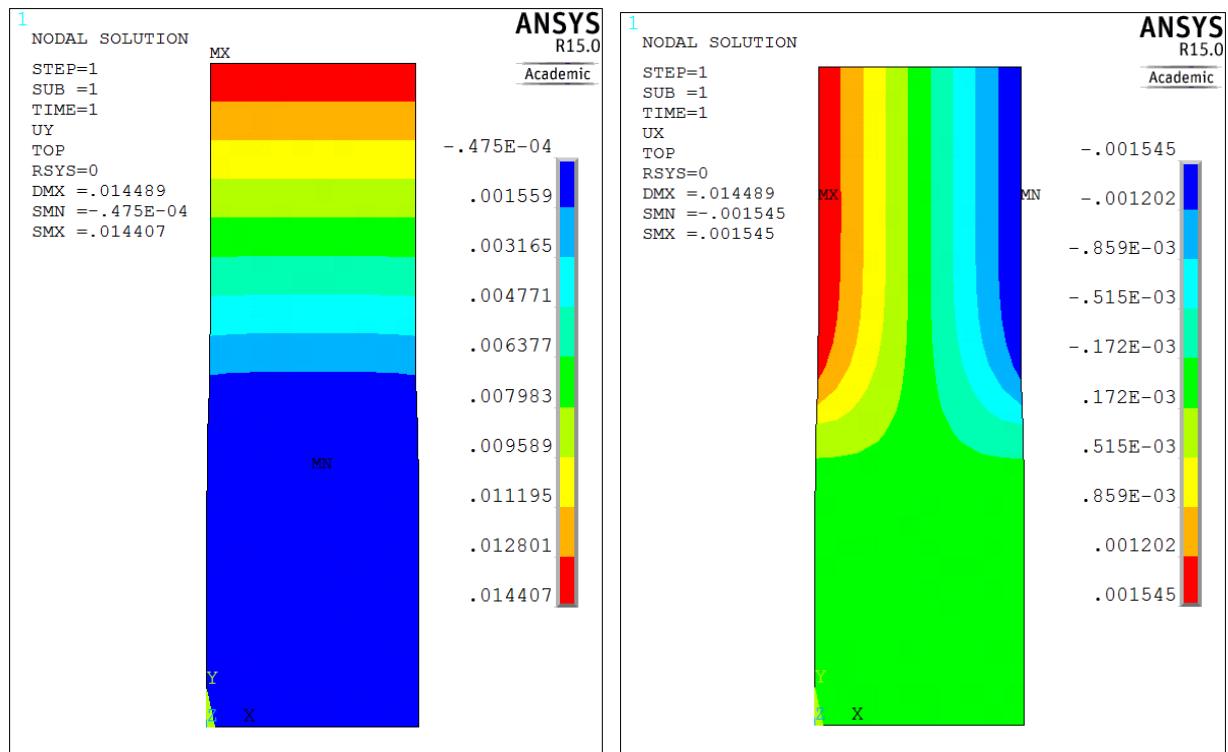


Figure 5-3: Deformation UY in longitudinal direction (left) and UX in transversal direction (right)

5.3 Results under consideration of assembly constraints

For the optimization with assembly constraints the same starting parameters are used shown in Table 5-3. It is expected that the same constraints for the failure criteria are active namely compression buckling for panel 1 and strength in panel 2. Furthermore the two thickness values and the LP sets of the panels should be held closely together forced by the assembly constraints. The results of the optimized panels with assembly constraints are shown in Table 5-5. The expected constraints of the particular panel are active again. Based on the difference values shown in the last column of Table 5-5, it can be observed that the design parameters are held close together and do not diverge as it was the case for the optimization without assembly constraints (see Table 5-4). This leads to a higher thickness of panel 2 and consequently to a structure with 3.5 kg more weight. Both assembly constraints are active, the one for the taper ratio as well as the one restricting the feasible domain of the $\Delta V_{[1,2]}^{*A,D}$ parameters.

Table 5-5: Results of the optimized panels with assembly constraints

Result	Panel 1	Panel 2	Difference
V_1^{*A}	0.14	0.21	0.07
V_2^{*A}	0.06	0.39	0.33
V_1^{*D}	-0.01	0.12	0.13
V_2^{*D}	-0.70	0.00	0.70
$T [mm]$	4.09	3.40	0.69
Active failure constraint	Compression buckling	Strength	
Active assembly constraint	Both		
Structural mass [kg]	17.86		

Figure 5-4 shows how the optimum LP sets of panel 1 and 2 changes when taken into account the assembly constraints. The optimum of panel 1 is shifted from the lower corner of the LP domain ($\pm 45^\circ$ plies) in the direction of zero especially visible in the domain $V_2^{*A} = f(V_1^{*A})$. This new optimum is taken as a reference and a center point to plot the feasible domain of the delta values (green envelope) around it. The originally domain based on absolute delta values is mirrored at the vertical and horizontal axis (green dotted lines) that goes through the optimum of panel 1 to indicate the permitted positions of the optimal panel 2. The optimum of panel 2 is shifted from the upper right corner of the LP domain (black dotted line) to the border of the feasible domain of the delta values which confirms the activity of the assembly constraint. It has to be noted that Figure 5-4 shows only two-dimensional sectional views of the originally four-dimensional feasible domain. The optimal point do not have to touch the border of the domain at all hyperplanes simultaneously. This explains why the corresponding point in the domain $V_2^{*D} = f(V_1^{*D})$ is not located directly on the border line but only close to it.

By comparing the feasible domains of the LPs (black dotted line) and the delta values (green envelope) it might be surprising that the one of the delta values extends beyond the LP domain. The assembly constraint formulation is based on the maximum possible differences and does not take into account the absolute position of the LPs. The equations that define the assembly constraints are determined based on the material properties and a thickness range before the optimization is started. Therefore the absolute positions of the LPs arising during the optimization cannot be considered. The LP sets of the complete feasible domain are used instead. The LP constraints for each panel specified in equations (3-20) to (3-38) ensure that the feasible domain of the LPs is not violated.

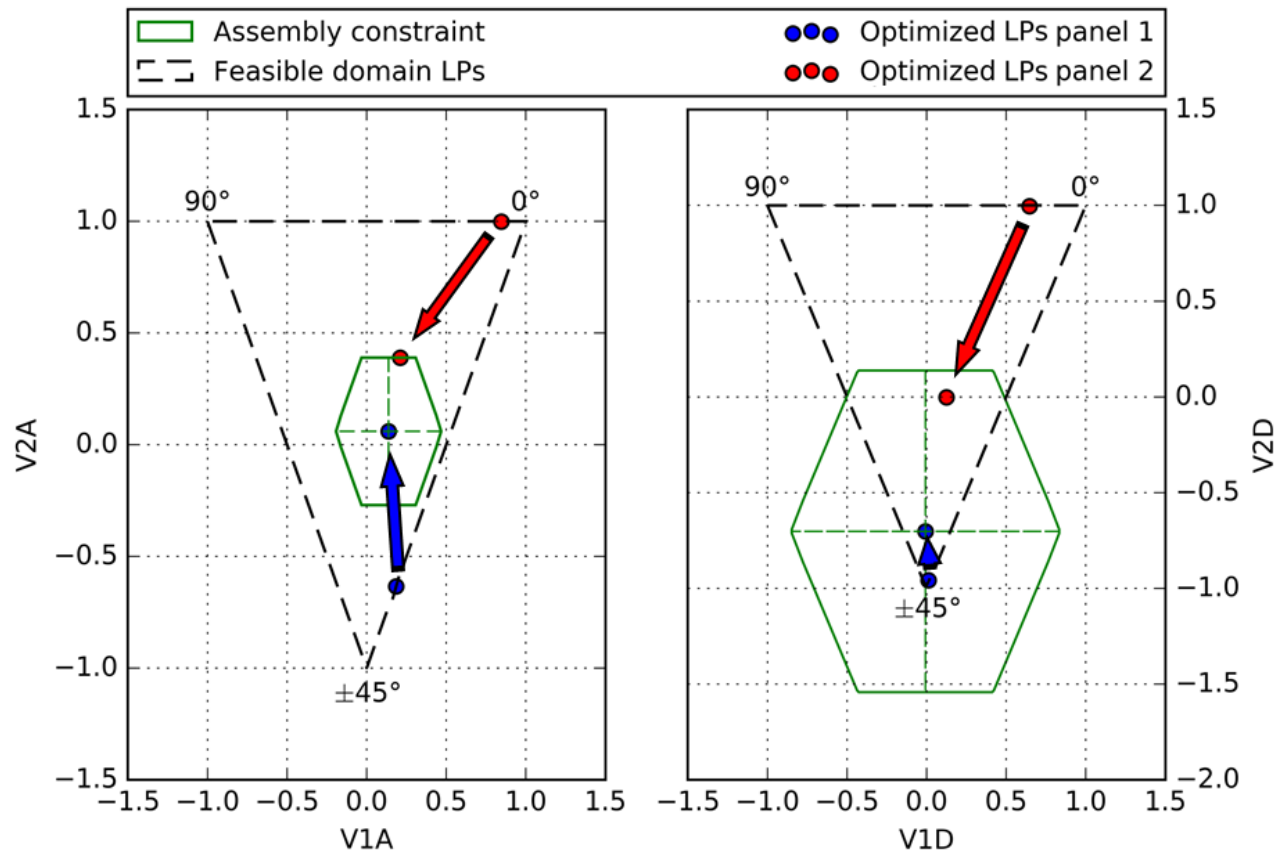


Figure 5-4: Change in the optimal LPs due to the assembly constraints

5.4 Conversion to discrete stacking sequences

The optimal set of LPs of each panel obtained in the previous sections has to be transformed back to a discrete stacking sequence. The detailed optimization process how to find the best matching stackings of the two panels is not part of the present thesis. A simplified approach based on the Brute Force method is presented in this section.

The panel thickness is used to determine the total number of plies. In the present case an even number is required to guarantee the symmetry of the laminate. With the optimal values $V_{[1,2]}^{*A}$ and the material invariants the $[A]$ -matrix is calculated. Based on the three diagonal values A_{11}, A_{22}, A_{66} , the discrete number of $0^\circ, 90^\circ$ and $\pm 45^\circ$ plies can be determined by solving the linear system of equations with 3 equations and the 3 unknowns. n_0 denotes the unknown number of 0° plies and $(\bar{Q}_{11})_0$ the reduced stiffness of one 0° ply transformed into the global longitudinal direction as already introduced in section 3.1.

$$\begin{aligned} A_{11} &= n_0 (\bar{Q}_{11})_0 + n_{45} (\bar{Q}_{11})_{45} + n_{90} (\bar{Q}_{11})_{90} \\ A_{22} &= n_0 (\bar{Q}_{22})_0 + n_{45} (\bar{Q}_{22})_{45} + n_{90} (\bar{Q}_{22})_{90} \\ A_{66} &= n_0 (\bar{Q}_{66})_0 + n_{45} (\bar{Q}_{66})_{45} + n_{90} (\bar{Q}_{66})_{90} \end{aligned} \quad (5-1)$$

The resulting numbers $0^\circ, 90^\circ$ and $\pm 45^\circ$ plies are floating point numbers and have to be rounded to even integer numbers. Thereby the total number of plies has to be fulfilled. Due to the fact that the process of rounding is not unique several combinations of even numbers of $0^\circ, 90^\circ$ and $\pm 45^\circ$ plies are created. The combination that fits best to the $[A]$ -matrix of the optimum values is used. Based on the number of $0^\circ, 90^\circ$ and $\pm 45^\circ$ plies all possible stackings are generated. For every stacking the LPs $V_{[1,2]}^{*D}$ are determined and compared to the optimal values. To have only one value as an indicator how close the LPs of the current stacking are, the sum of the absolute difference values are used as shown in the following equation.

$$sumOfDiff = abs((V_1^{*D})_{Stacking} - (V_1^{*D})_{Opt}) + abs((V_2^{*D})_{Stacking} - (V_2^{*D})_{Opt}) \quad (5-2)$$

The LPs $V_{[1,2]}^{*A}$ of the stackings with the 50 smallest sums of the absolute differences are all located around the optimum points as shown in the domain $V_2^{*D} = f(V_1^{*D})$ of Figure 5-5. It has to be noted that all stackings have the same number of $0^\circ, 90^\circ$ and $\pm 45^\circ$ plies (as calculated above) and therefor the same LPs $V_{[1,2]}^{*A}$ plotted in the domain $V_2^{*A} = f(V_1^{*A})$ of Figure 5-5. For the pressure loaded panel 1 the point of the discrete stacking is on the conservative side oriented in the direction of $\pm 45^\circ$ plies to prevent compression buckling. For the tension loaded panel 2 the conservative side would be right above the optimum in direction of the 0° plies. The point of the discrete stacking is located below the optimum which is assessed as unproblematic due to the round up to an even number of plies which results in a higher panel thickness.

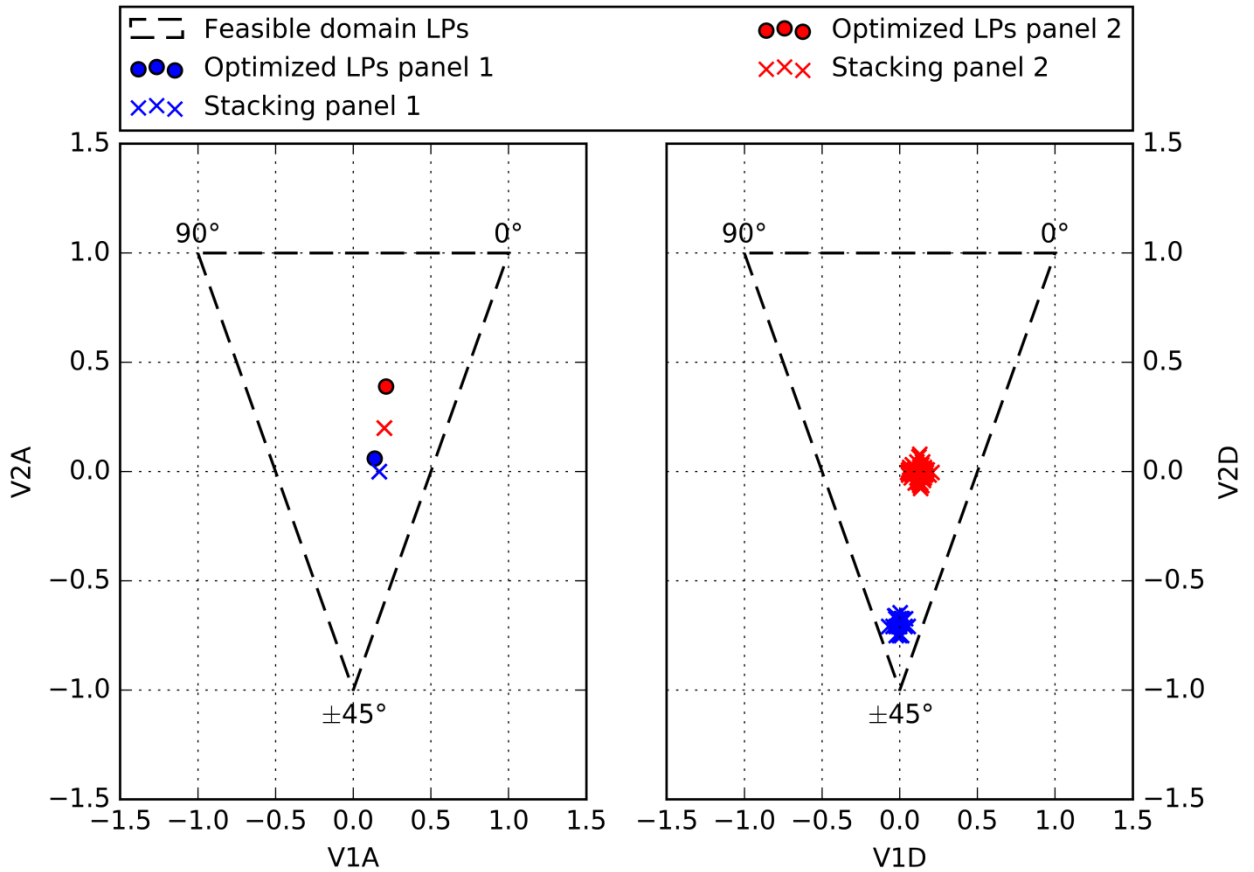


Figure 5-5: Back-transformation of the optimum LPs to discrete stackings

Figure 5-6 shows two stackings for the panels that were found among the 50 points that are closest to the optimum. It can be seen that all plies of the thinner laminate are also part of the thicker one which indicates that the blending rule is fulfilled. The number of continuous plies is 16 which constitutes a percentage of 67% with respect to the thicker laminate with 24 plies. The required ply continuity was given with 60%.

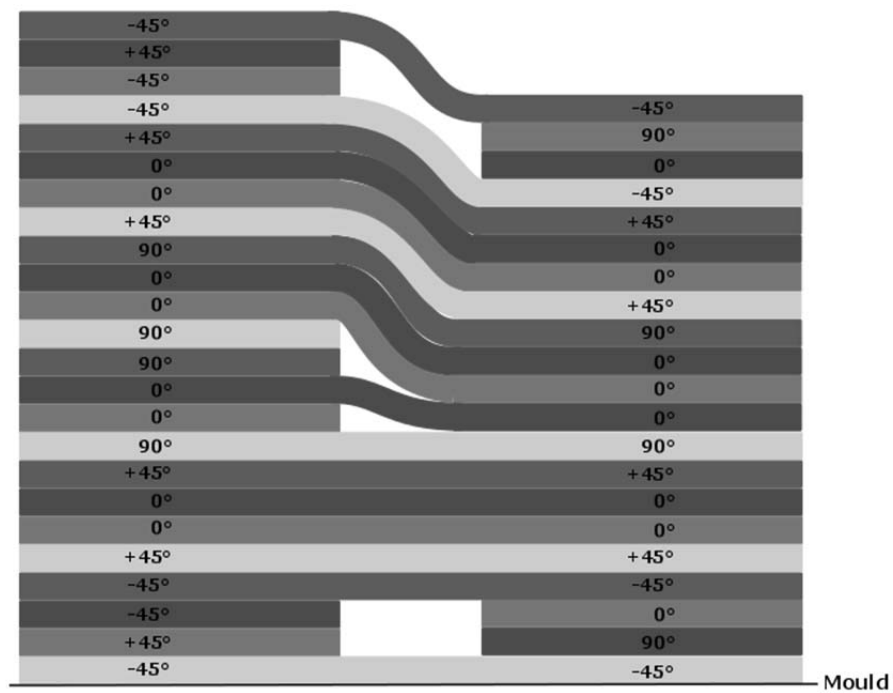


Figure 5-6: Discrete stacking sequences obtained for the two optimized panels under consideration of assembly constraints

Figure 5-7 shows the found stackings for the optimized panels without assembly constraints that match the optimum LP set. It can be observed that neither the ply continuity (only 4 continuous plies) nor the blending rule is fulfilled which is obvious when comparing the locations of the optimum LP sets of panel 1 and 2 shown in Figure 5-2.

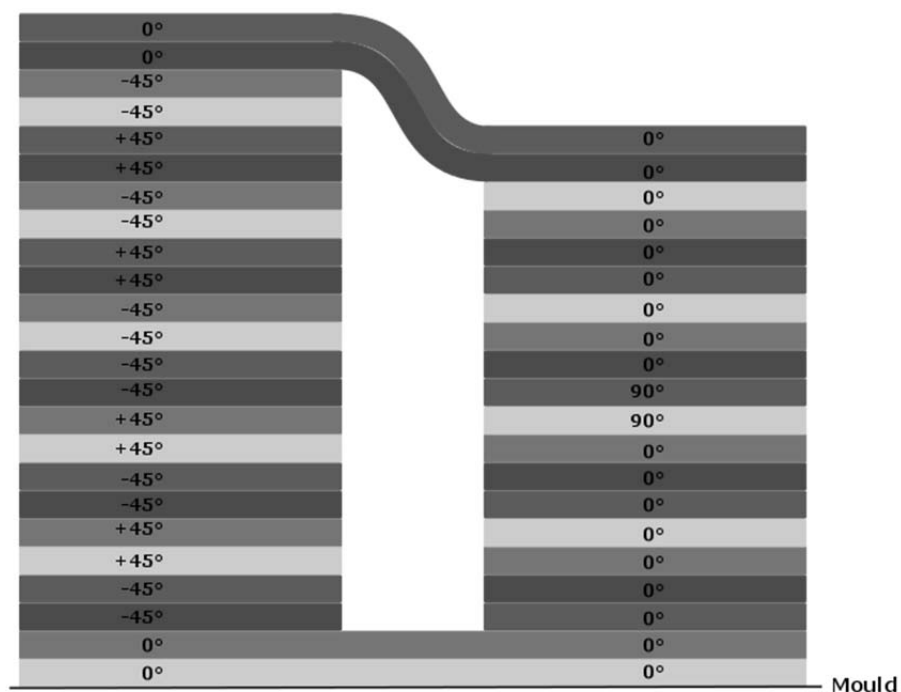


Figure 5-7: Discrete stacking sequences obtained for the two optimized panels without assembly constraints

For the optimization with assembly constraints it can be concluded that for both panels discrete stackings could be generated matching the optimum LPs with a sufficient precision and fulfilling the selected design rules at the same time.

6. Conclusion and Outlook

In the present thesis a design criterion was formulated based on selected design rules in thickness as well as in longitudinal direction. Thereby the approaches from Liu et al. [1] and Adams et al. [2] were used to combine a required ply continuity with laminate blending between two neighbouring panels. The design criterion was used to define assembly constraints for the optimization process VErSO that uses the laminate thickness and the lamination parameters as continuous design variables. The assembly constraints interrelate the lamination parameters of two adjacent panels with the help of convex hulls for the four-dimensional parameter space $\Delta V_{[1,2]}^{*A,D}$. The coefficients that describe the hyperplanes of the convex hull are used as linear constraint equations. It turned out that the size of the feasible domain is significantly smaller in comparison to the analytical approach developed by Macquart et al. [3]. The computational effort of the presented method is higher but needs to be carried out only once and that is outside of the optimization process.

A structure with two panels (optimization regions) was used to compare the results with and without the usage of assembly constraints. The boundary and load conditions of the panels were selected deliberately to obtain two divergent design parameter sets and different active failure criteria. The reference results without assembly constraints showed for the pressure loaded panel 1 an optimized parameter set to avoid failure due to compression buckling, whereas the tension loaded panel 2 got an optimized parameter set to prevent a failure of the strength. These two optimal points were located at completely different positions within the LP domain which correspond to completely different stackings that do not fulfill the selected design rules. The manufacturability of the structure is therefore not given. Applying the assembly constraints, the optimized parameter sets were significantly closer together. During the back-transformation of the LPs based on a Brute Force method, two discrete stackings could be obtained that fulfill the selected design rules. The manufacturability of the structure is given but with a weight penalty that has to be taken into account during performance computations already within the preliminary design phase.

The next logical step is the application of the method on a larger structure like a wind turbine blade or an aircraft wing. Due to the discretization of the structure, a high number of optimization regions will occur. Therefore it is useful to determine the permitted taper ratio and the allowable step in thickness direction of a continuous ply automatically based on the geometrical size of the optimization region. The speed of the back-transformation into discrete stackings can be increased with the help of a genetic algorithm. The algorithm uses a fitness function that evaluates how close are the parameters of a stacking to the optimal found parameter set under consideration of the design rules.

In the present work analytical LP constraints of Diaconu et al. ([21],[22]) shown in equations (3-20) to (3-38) were used. The calculation of the LP constraints and the assembly constraints can be combined in the future within the presented method. For a selected material the computation of the feasible domains for the LPs and their delta values based on the hyperplane coefficients can be done in one step in advance of the optimization. The constraints of Diaconu are restricted to symmetric and balanced laminates with 0°, 45° and 90° plies. The presented method allows the usage of arbitrary ply angles. Furthermore additional design rules in thickness and in longitudinal direction can be easily implemented.

For the application of structures where the usage of multiaxial fabrics is intended (e.g. wind turbine blades) the present process can be adapted quickly. The lamination parameters can be determined in the same way by just clustering the corresponding plies to one fabric ply which increases the permitted taper

ratio and the allowable step in thickness direction of a continuous ply. The present process is therefore fully transferable to multiaxial fabrics.

7. References

- [1] B. Liu and R. T. Haftka, "Composite Wing Structural Design Optimization with Continuity Constraints", Proceedings of the 42nd AIAA/ASME/ASCE/AHS/ASC Structures, Structural Dynamics and Materials Conference Seattle, WA, USA, 2001
- [2] D. B. Adams, L. T. Watson, Z. Gürdal, and C. M. Anderson-Cook, "Genetic Algorithm Optimization and Blending of Composite Laminates by Locally Reducing Laminate Thickness", *Advanced Engineering Software*, vol. 35, no. 1, pp. 35–43, 2004
- [3] T. Macquart, M. T. Bordogna, P. Lancelot, and R. De Breuker, "Derivation and application of blending constraints in lamination parameter space for composite optimisation", *Composite Structures*, Vol. 135, pp. 224–235, 2016
- [4] "HyperSizer Release 7.1.43", Collier Resesarch Corporation, 2014
- [5] M. C.-Y. Niu, "Composite Airframe Structures", 1st edition, 1992
- [6] US Department of Defense, "MIL-HDBK-17-3F Composite Materials Handbook - Volume 3: Polymer Matrix Composites, Materials Usage, Design and Analysis", vol. 3, 2002
- [7] J. A. Bailie, R. P. Ley, and A. Pasricha, "A Summary and Review of Composite Laminate Design Guidelines", NASA Contract NAS1-19347, 1997
- [8] R. M. Jones, "Mechanics of Composite Materials", London, Taylor & Francis, 1999
- [9] R. B. Pipes, "Interlaminar Stresses in Composite Laminates under Uniform Axial Extension", *Journal Composite Materials*, vol. 4, pp. 538–548, 1970
- [10] Structure Academy AIRBUS, "TCT - Transnational Composite Training Design", pp. 383–473, 2011
- [11] DNVGL and S. Pansart, "DNVGL-ST-0376 Rotor Blades for Wind Turbines", 2015
- [12] "www.smartblades.info"
- [13] G. Bir and P. Migliore, "Preliminary Structural Design of Composite Blades for Two- and Three-Blade Rotors", Colorado, 2004
- [14] D. S. Cairns, J. F. Mandell, M. E. Scott, and J. Z. Maccagnano, "Design considerations for ply drops in composite wind turbine blades", in 35th Aerospace Sciences Meeting and Exhibit, 1997
- [15] S. W. Tsai and N. J. Pagano, "Invariant Properties of Composite Materials," in *Composite Materials Workshop*, St. Louis Technomic, pp. 233–253, 1968
- [16] G. N. Vanderplaats, "Multidiscipline Design Optimization", 1st edition, Monterey, 2007
- [17] M. Miki, "A Graphical Method for Designing Fibrous Laminated Composites with Required In-Plane Stiffness", *Trans. JSCM*, vol. 9, pp. 51–55, 1983
- [18] M. Miki and Y. Sugiyama, "Optimum Design of Laminated Composite Plates Using Lamination Parameters", *AIAA Journal*, vol. 31, no. 5, pp. 921–922, 1993
- [19] H. Fukunaga and H. Sekine, "Stiffness Design Method of Symmetric Laminates Using Lamination Parameters", *AIAA Journal*, vol. 30, no. 11, pp. 2791–2793, 1991
- [20] C. G. Diaconu, M. Sato, and H. Sekine, "Feasible Region in General Design Space of Lamination Parameters for Laminated Composites", *AIAA Journal*, vol. 40, no. 3, pp. 559–565, 2002
- [21] C. G. Diaconu and H. Sekine, "Layup Optimization for Buckling of Laminated Composite Shells with Restricted Layer Angles", *AIAA Journal*, vol. 42, no. 10, pp. 2153–2163, 2004

-
- [22] C. G. Diaconu, M. Sato, and H. Sekine, "Buckling Characteristics and Layup Optimization of Long Laminated Composite Cylindrical Shells Subjected to Combined Loads Using Lamination Parameters", *Composite Structures*, vol. 58, no. 4, pp. 423–433, 2002
 - [23] VDI, "VDI 2014-3 Development of FRP Components - Analysis", Düsseldorf, 2006
 - [24] S. Dähne, "Auslegung und Optimierung von versteiften Hautstrukturen aus Faserverbundwerkstoffen im Vorentwurf", TU Berlin, 2013
 - [25] S. T. Ijsselmuiden, M. M. Abdalla, and Z. Gürdal, "Implementation of Strength-Based Failure Criteria in the Lamination Parameter Design Space", *AIAA Journal*, vol. 46, no. 7, pp. 1826–1834, 2008
 - [26] H. M. Adelman and R. T. Haftka, "Sensitivity Analysis of Discrete Structural Systems", *AIAA Journal*, vol. 24, no. 5, pp. 823–832, 1986
 - [27] S. G. Johnson, "The NLOpt nonlinear-optimization package", <http://ab-initio.mit.edu/nlopt>
 - [28] K. Svanberg, "A Class of Globally Convergent Optimization Methods Based on Conservative Convex Separable Approximations", *SIAM Journal Optimization*, vol. 12, no. 2, pp. 555–573, 2002
 - [29] C. B. Barber and D. P. Dobkin, "The Quickhull Algorithm for Convex Hulls", vol. 22, no. 4, pp. 469–483, 1996
 - [30] "ANSYS Mechanical APDL Release 15.0", ANSYS Inc., 2013
 - [31] L. Marin, D. Trias, P. Badallo, G. Rus, and J. A. Mayugo, "Optimization of composite stiffened panels under mechanical and hygrothermal loads using neural networks and genetic algorithms", *Composite Structures*, vol. 94, no. 11, pp. 3321–3326, 2012

8. Appendix

8.1 List of figures

Figure 2-1: Symmetric laminate with four plies under axial loading [9]	5
Figure 2-2: Right part of the outer ply extracted as a free body.....	6
Figure 3-1: Sign convention for the cutting forces on a) the membrane- and b) the plate element	13
Figure 3-2: Ply numbering and -positioning within the laminate.....	14
Figure 3-3: Decomposition of the reduced stiffness component [8]	15
Figure 3-4: Physical example (above) and process (below) for a gradient-based optimization [16].....	17
Figure 3-5: Two-variable problem with a one-dimensional search [16]	19
Figure 3-6: A convex (a) and a non-convex (b) set of points.....	20
Figure 3-7: Feasible domain for either the in- or out-of-plane LPs.....	21
Figure 3-8: Construction of a design point representing multiple laminates	22
Figure 3-9: Discrete design points of a 4-ply laminate (left), Complete feasible domain of any symmetric laminate with ply angles out of the set of $0^\circ, 45^\circ$ and 90°	23
Figure 3-10: Feasible domain of a desired lamination parameter set [20]	24
Figure 3-11: Proof if a LP set belongs to the feasible domain [20]	26
Figure 3-12: Definition of the safety factor for the strength criterion.....	29
Figure 3-13: Initialization of the optimization.....	33
Figure 3-14: Object model structure and indexing of the design parameters.....	33
Figure 3-15: Running optimization process in VErSO.....	34
Figure 4-1: Stacking sequence continuity [1]	35
Figure 4-2: Guide based design completely outwardly blended [2]	36
Figure 4-3: Normalised change in lamination parameter V1 due to one ply-drop [3].....	37
Figure 4-4: Tapering areas based on a taper slope (left) summarized to a discrete thickness step (right) ..	38
Figure 4-5: Blended laminate with 12 plies, 50% ply continuity and 50% taper ratio	39
Figure 4-6: Blended laminate with 50% ply continuity and 50% taper ratio, new definition of continuous plies	39
Figure 4-7: Comparison between the envelope of the ΔV_{\max} values and the convex hull for a laminate configuration with 12 plies a taper ratio of 0.5 and a required ply continuity of 0.5	42
Figure 4-8: Number of hyperplanes and volume size over laminate thickness	43
Figure 4-9: Feasible domains for 12, 16 and 20 plies with a taper ratio of 0.2 and a required ply continuity of 0.6.....	44
Figure 4-10: Feasible domain for 12 plies with a taper ratio of 0.5 and a required ply continuity of 0.0	45

Figure 4-11: Comparison between Macquart's feasible domain and the convex hull for a laminate configuration with 12 plies a taper ratio of 0.2 and a required ply continuity of 0.6.....	46
Figure 5-1: FE-model	48
Figure 5-2: LP set of the individually optimized panels.....	50
Figure 5-3: Deformation UY in longitudinal direction (left) and UX in transversal direction (right).....	51
Figure 5-4: Change in the optimal LPs due to the assembly constraints	52
Figure 5-5: Back-transformation of the optimum LPs to discrete stackings.....	54
Figure 5-6: Discrete stacking sequences obtained for the two optimized panels under consideration of assembly constraints	55
Figure 5-7: Discrete stacking sequences obtained for the two optimized panels without assembly constraints.....	55

8.2 List of tables

Table 1-1: List of Symbols and Units	III
Table 1-2: Indices.....	IV
Table 1-3: Terms and abbreviations used	IV
Table 2-1: Design rules in thickness direction used in the aircraft industry	8
Table 2-2: Design rules in longitudinal direction used in the aircraft industry.....	9
Table 2-3 Design rules used in the wind power industry	11
Table 3-1: Matrix containing the gradients.....	31
Table 4-1: Exemplary process to obtain the changes in LPs for the reduced stackings of one original stacking.....	40
Table 5-1: Model data	49
Table 5-2: Material data	49
Table 5-3: Starting parameters of the optimizer.....	49
Table 5-4: Results of the individually optimized panels.....	50
Table 5-5: Results of the optimized panels with assembly constraints	51